END

FILMED

DTIC

MICROCOPY RESOLUTION TEST CHART

NATIONAL BUREAU OF STANDARDS-1963-A

PHOTOLUMINESCENCE STUDY OF N-TYPE

THERMAL CONVERSION IN SI GaAs

THESIS

AFIT/GEO/PH/82D-3
John A. Guillen
Captain   USAF

DEPARTMENT OF THE AIR FORCE

AIR UNIVERSITY (ATC)

AIR FORCE INSTITUTE OF TECHNOLOGY

Wright-Patterson Air Force Base, Ohio

83 02 022 096

SECURITY CLASSIFICATION OF THIS PAGE *(When Data Entered)*

REPORT DOCUMENTATION PAGE		READ INSTRUCTIONS BEFORE COMPLETING FORM
1. REPORT NUMBER AFIT/GEO/PH/82D-3	2. GOVT ACCESSION NO. AD-A124 772	3. RECIPIENT'S CATALOG NUMBER
4. TITLE *(and Subtitle)* PHOTOLUMINESCENCE STUDY OF N-TYPE THERMAL CONVERSION IN SEMI-INSULATING GaAs		5. TYPE OF REPORT & PERIOD COVERED MS Thesis
		6. PERFORMING ORG. REPORT NUMBER
7. AUTHOR(*s*) JOHN A. GUILLEN Captain USAF		8. CONTRACT OR GRANT NUMBER(*s*)
9. PERFORMING ORGANIZATION NAME AND ADDRESS Air Force Institute of Technology (AFIT-EN) Wright-Patterson AFB OH 43433		10. PROGRAM ELEMENT, PROJECT, TASK AREA & WORK UNIT NUMBERS
11. CONTROLLING OFFICE NAME AND ADDRESS Air Force Avionics Laboratory (AFWAL/AADR) Wright-Patterson AFB OH 45433		12. REPORT DATE December 1982
		13. NUMBER OF PAGES 72
14. MONITORING AGENCY NAME & ADDRESS *(if different from Controlling Office)*		15. SECURITY CLASS. *(of this report)* UNCLASSIFIED
		15a. DECLASSIFICATION/DOWNGRADING SCHEDULE

16. DISTRIBUTION STATEMENT *(of this Report)*

Approved for Public Release; Distribution Unlimited

17. DISTRIBUTION STATEMENT *(of the abstract entered in Block 20, if different from Report)*

18. SUPPLEMENTARY NOTES

Approved for public release: IAW AFR 190-17.

LYNN E. WOLAVER
Dean for Research and Professional Development
Air Force Institute of Technology (ATC)
Wright-Patterson AFB OH 45433

19 JAN 1983

19. KEY WORDS *(Continue on reverse side if necessary and identify by block number)*

Photoluminescence

Gallium Arsenide

Thermal Conversion

20. ABSTRACT *(Continue on reverse side if necessary and identify by block number)*

Chromium doped SI GaAs samples annealed at temperatures from 650° C to 950° C were examined for n-type thermal conversion. From Van der Pauw Hall measurements, it was determined that the samples annealed at 850° C, 900° C and 950° C thermally converted. These converted samples were then subjected to resistivity profile measurements to determine the extent of the thermally converted layer. Depth resolved photoluminescence was also used to observe

(Continued on Reverse)

DD ᶠᴼᴿᴹ 1473   EDITION OF 1 NOV 65 IS OBSOLETE

BLOCK 20: Abstract (Cont'd)

changes in the spectra as surface layers from the converted samples were removed. Although changes in the spectra were observed, none could be related to thermal conversion.

AFIT/GEO/PH/82D-3

PHOTOLUMINESCENCE STUDY OF N-TYPE

THERMAL CONVERSION IN SI GaAs

THESIS

John A. Guillen
AFIT/GEO/PH/82D-3   Captain   USAF

DTIC
ELECTE
S FEB 2 3 1983
D
E

PHOTOLUMINESCENCE STUDY OF N-TYPE

THERMAL CONVERSION IN SI GaAs

THESIS

Presented to the Faculty of the School of Engineering

of the Air Force Institute of Technology

Air University

in Partial Fulfillment of the

Requirements for the Degree of

Master of Science

by

John A. Guillen, B.S.E.E.

Captain   USAF

Graduate Electro-Optics

December 1982

Approved for Public Release; Distribution Unlimited

Preface

The completion of this thesis project was a very beneficial portion of my training at the Air Force Institute of Technology. However, it would not have been possible without the advice and assistance of the many people at AFIT and the Air Force Avionics Laboratory.

I would like to express my gratitude to my thesis advisor, Dr. Robert L. Hengehold, for his continued guidance throughout this effort. I would also like to thank Dr. Yoon Soo Park of the Avionics Laboratory for providing the samples used in this thesis. I also want to thank Dr. Yung Kee Yeo of the Avionics Laboratory for his help in performing Van der Pauw measurements of the samples. Additional thanks go to fellow AFIT student, Captain Yong Yun Kim, Republic of Korea Army, for his help in preparing the samples for Van der Pauw measurements. Thanks also to Don Elworth, Ron Gabriel, and George Gergal of the AFIT Physics Laboratory staff for their technical assistance. I would also like to thank Charles Geesner of the Avionics Laboratory for his assistance in capping and annealing the samples. Mr. Jack Capehert, Lt Ron Benner and Deborah Taylor in the Analog-Hybrid section of the ASD Computer Center were very helpful in converting the data on paper tape to cards for generating the plots which appear in this thesis. I would also like to express my appreciation to Sharon Gabriel for her typing of this thesis. Finally, I would like to thank my parents for their support during the course of this project.

John A. Guillen

ii

Contents

Contents (Cont'd)

List of Figures

List of Tables

AFIT/GEO/PH/82D-3

Abstract

Chromium doped SI GaAs samples annealed at temperatures from 650° C to 950° C were examined for n-type thermal conversion. From Van der Pauw Hall measurements, it was determined that the samples annealed at 850° C, 900° C and 950° C thermally converted. These converted samples were then subjected to resistivity profile measurements to determine the extent of the thermally converted layer. Depth resolved photoluminescence was also used to observe changes in the spectra as surface layers from the converted samples were removed. Although changes in the spectra were observed, none could be related to thermal conversion.

PHOTOLUMINESCENCE STUDY OF N-TYPE

THERMAL CONVERSION IN SEMI-INSULATING GaAs

I. Introduction

The doping of gallium arsenide with chromium (GaAs:Cr) produces high resistivity material (semi-insulating) which is used as a substrate for the fabrication of integrated circuit (IC) devices (Ref 1:1). The first step in the production of these devices requires the heating of the substrate to a working temperature. If the substrate is ion-implanted, then high temperature annealing is required to remove any damage caused by the implantation procedure (Ref 2:220). Several studies have determined that these heat treatments result in the formation of low resistivity p-type or n-type layers in the surface region of the gallium arsenide. This phenomenon, known as thermal conversion, reduces the performance of IC devices (Ref 3:8226).

For many years, the Electronics Research Branch of the Air Force Avionics Laboratory (AFWAL/AADR) has been performing research on gallium arsenide for applications in reconnaissance and communication systems, high speed signal processing in electronic warfare and real-time digital radar (Ref 4:1). Gallium arsenide, which is a III-V group semiconductor, has characteristics which lend themselves to the aforementioned applications. Therefore, due to the extensive use and

1

application of semi-insulating (SI) GaAs as a substrate, AFWAL/AADR has initiated research to determine the causes of thermal conversion.

Summary of Previous Work

Although the thermal conversion problem was first reported by J.T. Edmond and J.J. Wysocki in 1960 (Refs 5, 6), it was not until 1977 that Lum et al investigated this problem in Chromium (Cr)-doped semi-insulating (SI) GaAs. In their investigation, a sample of bulk Cr-doped SI GaAs was heat treated at 750° C for 2.75 hours in hydrogen (H_2) gas flow, resulting in p-type thermal conversion. It was theorized that heat-treating the GaAs produced arsenic (As) vacancies which were occupied by Group-IV impurities such as Carbon (C) or silicon (Si) acting as acceptors (Ref 7:1). In a paper later that year, Lum and Wieder investigated the heat treatment of Cr-doped SI GaAs wafers at 900° C in H_2 gas for one hour. In contrast to their previous study, Lum and Wieder determined that the converted surface layers were n-type rather than p-type. They attributed this type of conversion to the high density of C impurities localized on gallium (Ga) vacancies within the region of the surface layer. From these two studies, it was generally concluded that since Ga and As vacancies are thermally generated, and may be occupied by amphoteric impurities such as carbon, p-type or n-type conversion depends upon the thermal treatment conditions (Ref 8:213).

2

In 1977, Zucca performed a study on Cr-doped SI GaAs by annealing samples at temperatures between 700° C and 750° C in a H_2 gas environment. Heating the GaAs resulted in p-type surface layers. Zucca concluded that the formation of these surface layers was due to the presence of Manganese (Mn) impurities acting as acceptors. Zucca also concluded that impurity doping, aided by vacancy formation rather than the formation of isolated Ga or As vacancies, was the principal mechanism for p-type conversion for moderate heat treatment of Cr-doped Si GaAs (Ref 9:234). The results of Zucca correlated well with the investigation performed by Hallais et al in the same year.

In the study by Hallais et al, samples of Cr-doped SI GaAs were heated in H_2 gas at 750° C for 30 minutes. Although the p-type layers that formed were attributed to the presence of Mn impurities localized at Ga sites, there was no explanation given for the presence of manganese (Ref 2:226).

In a 1977 study by Ohno et al, samples of Cr-doped SI GaAs were heated in H_2 gas from 750° C to 950° C for two hours. It was concluded that p-type conversion was associated with the rapid outdiffusion of deep donors (oxygen) rather than with any other impurities. It is generally accepted that oxygen is introduced into the crystal when grown by the Czochlarski technique. If the concentration of deep acceptors (Chromium) is not high enough for compensation, then there is n-type conversion (Ref 3:8227-8228).

In 1977, Koschel et al attributed the formation of p-type layers in Cr-doped SI GaAs to a high density of carbon atoms (acceptors) within this layer. The samples were annealed in H_2 gas at 740° C for 100 minutes. From this study, it was concluded that during the annealing process, arsenic vacancies were created as a result of arsenic loss. These vacancies then diffused from the surface into the bulk of the crystal where they were occupied by carbon atoms (Ref 10:100).

Kasahara et al, in a 1979 study, suppressed the degree of thermal conversion in Cr-doped SI GaAs samples by annealing the samples at 850° C for 15 minutes under various arsenic partial pressures. Although all of the samples n-type converted, no specific reason for thermal conversion was proposed. However, it was noted that increased arsenic loss increases the degree of thermal conversion. For those samples that did not convert, it was suggested that the shallow donors present were completely compensated by sufficient chromium atoms (Ref 11:8230).

Klein et al in 1980 confirmed earlier results by Zucca and Hallais that p-type conversion in SI GaAs as a result of heat treatment at 740° C in H_2 gas was directly attributed to Mn acceptors localized on Ga sites. Unlike Zucca and Hallais, secondary-ion-mass spectrometry was used to show the presence of a significant Mn concentration in the surface layer that correlated with the p-type conversion. It was suggested that the Mn impurity was present in low concentration throughout the bulk of the material and that diffusion toward the surface

occurred during heating (Ref 12:4867). Anderson (Ref 13: 21-23, 58) contradicted these results by ruling out Mn as the cause for p-type thermal conversion.

In a 1980 study, Anderson annealed Cr-doped SI GaAs samples in H_2 gas at 850 C for 20 minutes. Manganese was ruled out because the photoluminescence due to this impurity was observed to come and go without affecting the electrical properties of the sample. Instead, Anderson associated conversion with the presence of silicon impurities.

Problem and Scope

The purpose of this study will be to investigate the cause of n-type thermal conversion in chromium doped semi-insulating GaAs using photoluminescence. Photoluminescence spectra of converted and unconverted samples, in conjunction with electrical profile measurements, will be used to identify the mechanisms of thermal conversion.

This problem is of particular interest since predominantly p-type conversion has been observed in SI GaAs rather than n-type. In addition, the problem of n-type conversion in SI GaAs has not been studied extensively.

II. Theory

This chapter contains a discussion of the relevant theory for this study. The topics discussed in this chapter are semi-conductor band theory, photoluminescence theory, and the theory of radiative and non-radiative recombination.

Semiconductor Band Theory

A semiconductor is a crystalline substance having an energy band structure consisting of a conduction band and valence band separated by an energy gap. At absolute zero, the semiconductor is essentially a perfect insulator since the conduction band is completely empty, whereas the valence band is completely filled. This is illustrated in Figure 1(a). At higher temperatures, a few electrons from the valence band acquire enough thermal energy to transverse the energy gap and become conduction electrons in the conduction band. In addition to the conduction band electrons, the empty states left behind in the valence band behave as positively charged particles (holes) and contribute to the conductivity of the material (Ref 14:257). This is illustrated in Figure 1(b). An intrinsic semiconductor is a material in which the conductivity is an inherent property of the material.

Impurities are often present in semiconductors. In the case of intrinsic semiconductors, impurity atoms may be
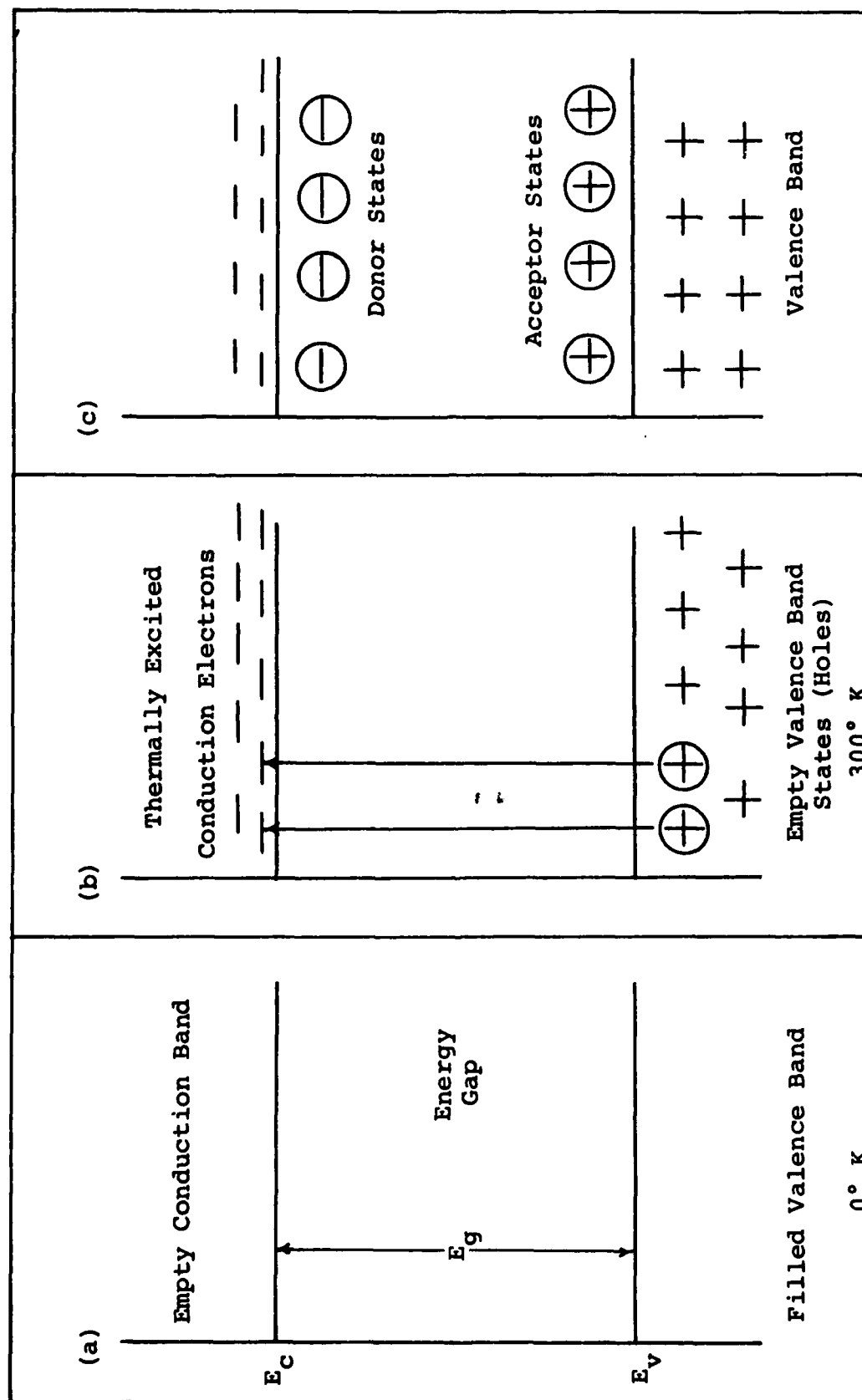
Figure 1. Conduction and Valence Bands of a Pure Semiconductor at (a) 0° K, (b) 300° K, Impurity Levels in a Doped Semiconductor, (c) (Ref 15:6).

7

introduced intentionally to increase the conductivity of the material. This process is known as doping. In other instances, impurities may be inherent to the semiconductor due to the nature of the growth process. In either case, when impurities are present, they may occupy lattice sites which would normally be occupied by atoms of the semiconductor. Depending upon the type of crystal and impurity present, the impurity becomes an acceptor (p-type) or a donor (n-type).

Acceptor impurities are referred to as p-type because they readily accept an electron, thus freeing up a mobile hole. Donor impurities are referred to as n-type because they donate an additional free electron to the crystal. For example, in GaAs, a tellurium atom on an arsenic site (Te_{As}) or a silicon atom on a gallium site (Si_{Ga}) are donor atoms because of the extra electrons they provide. On the other hand, a zinc atom on a gallium site (Zn_{Ga}) or a silicon atom on an arsenic site (Si_{As}) are termed acceptors because they provide less electrons then they replace. Impurities which can be located at either an As site or a Ga site are referred to as amphoteric impurities. A vacancy at a lattice site is termed an acceptor because the vacancy deprives the crystal of one electron per broken bond (Ref 16:8, 15:7). The electrons contributed by the donor atoms can be thought of as originating from donor states which lie within the energy gap just below the conduction band. Likewise, the holes contributed by the acceptor atoms can be thought of as originating from acceptor states just above the valence band.

Figure 1(c) depicts the donor and acceptor levels (Ref 14: 269). A semiconductor whose conductivity is determined predominantly by impurities (n-type or p-type) is referred to as an extrinsic semiconductor.

Compensation in an extrinsic semiconductor occurs when the number of donor and acceptor atoms are made equal. The material, therefore, behaves as an intrinsic semiconductor so far as electron and hole populations are concerned (Ref 14: 274). Compensation can be accomplished by the additional doping of donor or acceptor impurities. An example of compensation is in the production of semi-insulating GaAs.

As stated in Chapter I, high resistivity or semi-insulating GaAs is used for the fabrication of substrates. Gallium arsenide, when prepared by the Czochralski or Bridgman methods, usually contains n-type (donor) impurities. In order to offset the low resistivity due to these donor atoms, chromium is often introduced to increase the resistivity to values found in intrinsic semiconductors (Ref 17:95). The chromium atoms act as deep acceptors and those acceptors are compensated by the shallow donors. The chromium deep acceptor level is located near the middle of the energy gap (Refs 18:876; 17:96).

Photoluminescence Theory

Photoluminescence occurs when free carriers in a semiconductor recombine and emit their energy in the form of light.

9

Excitation to a non-equilibrium state is achieved by irradiating the system with light. During the photoluminescence process, three distinctive steps occur: (i) the creation of electron-hole pairs by absorption of the exciting light, (ii) radiative recombination of electron-hole pairs, and (iii) the escape of this radiation from the system. The greatest excitation of the sample is near the surface, creating electron-hole pairs that result in a carrier distribution which is both inhomogeneous and in non-equilibrium. In an attempt to regain homogeneity and equilibrium, these electron-hole pairs will diffuse away from the surface while being depleted by both radiative and non-radiative recombination processes (Refs 19:182; 15:8).

The radiative recombination process involves the release of energy in the form of photons. The energy from these transitions usually appears in the visible or near infrared region of the spectrum. In non-radiative recombination, energy is not released in the form of photons. Consequently, although photoluminescence studies can be used to observe radiative transitions directly, the non-radiative processes can only be deduced indirectly (Ref 20:300).

Radiative Recombination Processes

When electron-hole pairs recombine, the following types of radiative transitions are possible: (i) excitons, (ii) band-to-band, (iii) donor-to-valence band, (iv) conduction band-

to-acceptor, (v) donor-to-acceptor, and (vi) phonon-replicas. The radiative transitions (i)-(v) are illustrated in Figure 2.

Radiative recombinations can have either simple centers or complex centers. A simple center is defined as an impurity which sits on a Ga or As lattice site and contributes only one additional carrier to the binding. Since the activation energy of the single carrier bound to the impurity is close to that calculated from the hydrogen model, simple centers are often referred to as hydrogenic centers. For acceptors, this ionization energy is 34 meV, whereas for donors it is 5.2 meV (Ref 19:327). Table I lists the ionization energies for simple acceptor centers in GaAs. Some of the impurities listed have two or more ionization energies as determined by different studies. Ionization energies for simple donor centers determined by photoluminescence and absorption methods are listed in Table II. Complex centers are defined as levels which are too broad and too low in energy to be classified as simple centers (Ref 19:359).

Excitons. Electron-hole pairs generated in a pure semi-conductor by some sort of excitation at or near the band edges are referred to as free excitons. Free excitons are mobile and can thus wander through the crystal. Because of their mobility, exciton states do not have well defined energy levels and are usually placed near the conduction band edge (Ref (16:13).

11
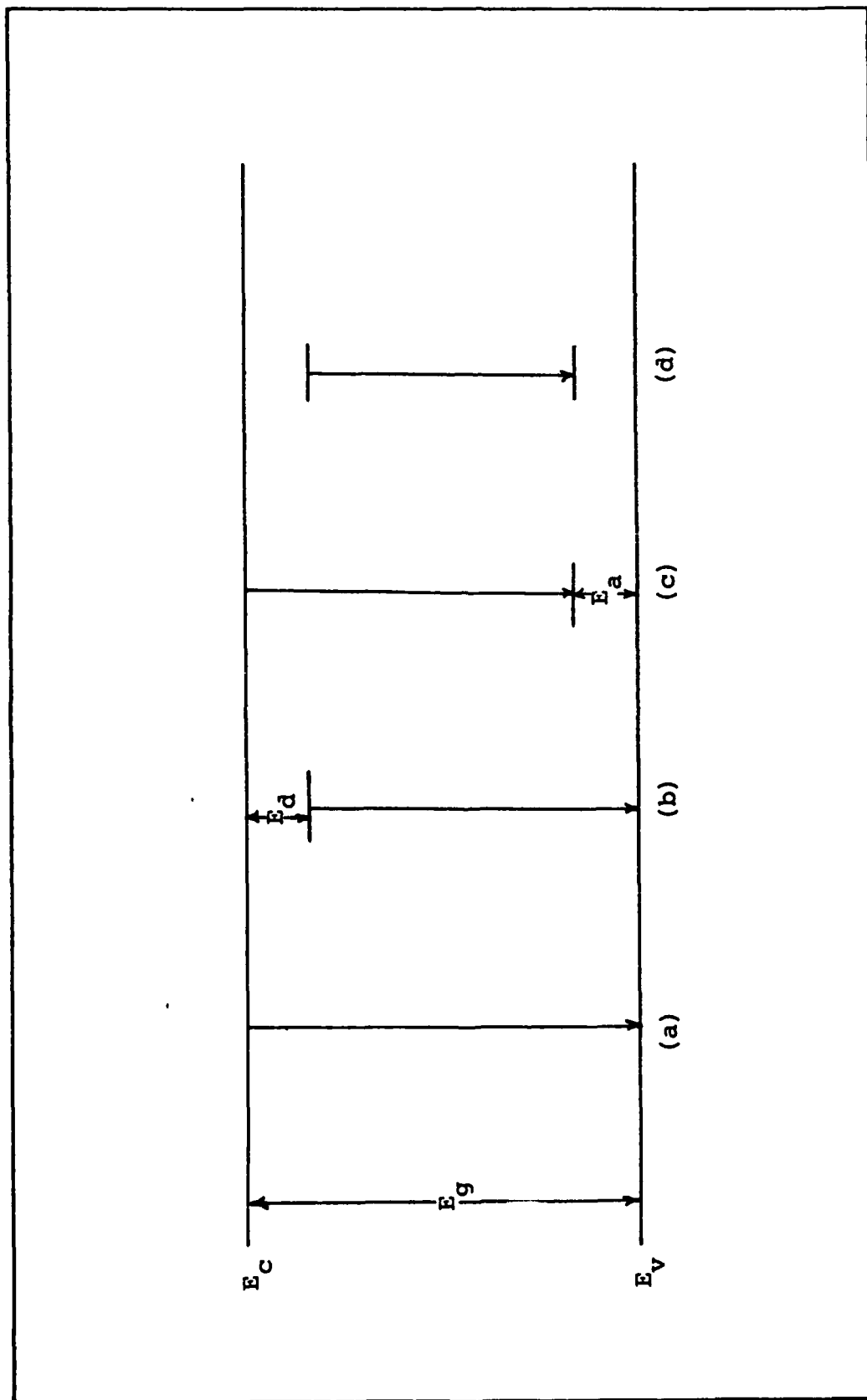
Figure 2.   Radiative Recombination Processes: (a) band-to-band, (b) donor-to-valence band, (c) conduction band-to-acceptor, (d) donor-to-acceptor. (Ref 20:295)

12

TABLE I (Ref 19:328)	
Simple Centers in GaAs	
Impurity	**Activation Energy (eV)**
Cadmium, Cd_{Ga}	0.0345
Cadmium, Cd_{Ga}	0.034
Zinc, Zn_{Ga}	0.030
Zinc, Zn_{Ga}	0.034
Zinc, Zn_{Ga}	0.032
Magnesium, Mg_{Ga}	0.030
Beryllium, Be_{Ga}	0.030
Carbon, C_{As}	0.020
Carbon, C_{As}	0.025
Silicon, Si_{As}	0.030
Germanium, Ge_{As}	0.030
Germanium, Ge_{As}	0.042
Germanium, Ge_{As}	0.038

	Activation Energy (meV)	
TABLE II (Ref 19:329) Simple Donor Centers in GaAs		
Impurity	Absorption-Photoconductivity	Photoluminescence
Silicon, Si_{Ga}	5.81	6.80
Germanium, Ge_{Ga}	6.08	----
Sulfur, S_{As}	6.10	----
Selenium, Se_{As}	5.89	6.10
Tellurium, Te_{As}	----	----

When an electron-hole pair recombines, a narrow spectral line is emitted (Ref 16:114). The energy of the emitted photon in a direct gap semiconductor, such as GaAs, is simply (Ref 16:114):

$$h\nu = E_g - E_x \pm E_k \tag{1}$$

where

$$E_g = \text{band gap energy}$$

$$E_x = \text{exciton binding energy}$$

14

$$E_k = \text{kinetic energy}$$

$$h\nu = \text{photon energy}$$

Excitonic complexes are formed when a free hole combines with either a neutral donor or a neutral acceptor. The free hole is then said to be "bound" to the neutral donor or acceptor (Ref 16:15). The following excitonic complexes have been observed in GaAs: (i) exciton bound to a neutron donor at 1.5145 eV, (ii) exciton bound to an ionized donor at 1.5133 eV, and (iii) exciton bound to a neutral acceptor at 1.5125 eV. An exciton bound to an ionized donor has not been observed in GaAs (Ref 19:341-342).

Band-to-Band Recombination. In less pure or less perfect crystals, local fields can break up an exciton into a free-hole and free-electron. These will then recombine in a band-to-band transition. In a direct gap semiconductor, a band-to-band transition is characterized by a temperature dependent high energy tail with a low energy edge cutoff at the band gap energy (Ref 16:124-125). The band gap for GaAs has been reported to be 1.5205 eV at 2° K (Ref 19:342).

Band-to-Impurity Recombination. Two types of band-to-impurity transitions are possible: (i) conduction-band-to-acceptor with emission at $h\nu = E_g - E_a$, and (ii) donor-to-valence band with emission at $h\nu = E_g - E_d$. These

15

types of deep transitions are illustrated in Figure 3.
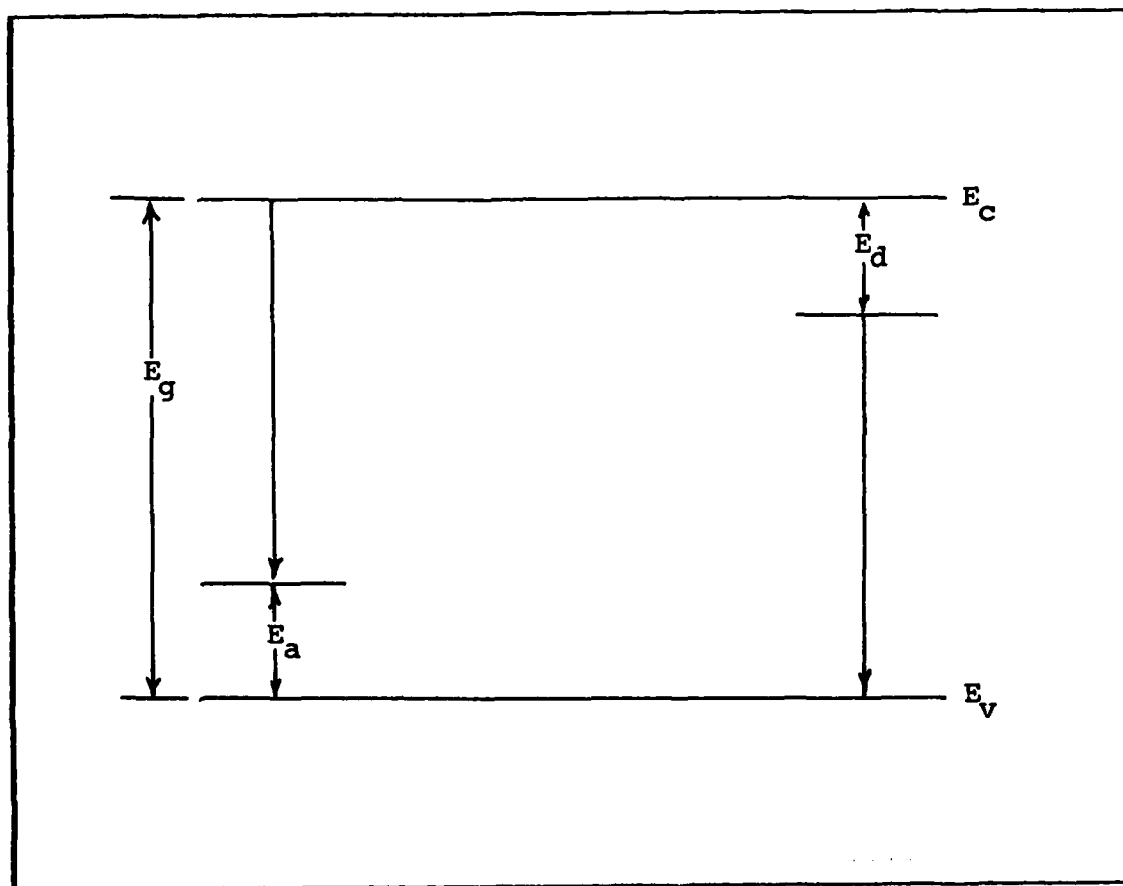
Figure 3. Radiative Transitions Between Band
and an Impurity State (Ref 16:133)

Shallower transitions to neutralize ionized donors or accep-

tors are possible and these types of transitions could be

radiative in the far infrared (Ref 16:131).

The observation of band-to-impurity transitions has

been limited to semiconductors with a low concentration of

impurities. However, for purer semiconductors, an exciton

transition would be more probable. As the impurity concen-

16

tration increases, the impurity band will merge with the nearest intrinsic band, thus decreasing the energy gap. The reduction in energy gap will cause the emission spectrum to broaden (Ref 16:134-136).

Donor-Acceptor Recombination. When donor and acceptor impurities are present, the recombination of an electron trapped on a donor with a hole on an acceptor results in luminescence given by the equation (Ref 19:335):

$$h\nu = E_g - E_A - E_D + \frac{q^2}{\varepsilon r} \tag{2}$$

where

E_g = band gap energv

q = electronic charge

ε = dielectric constant

r = separation between impurities

E_A = acceptor binding energy

E_D = donor binding energy

Since substitutional donor and acceptor impurities occupy lattice sites, and r varies in a discrete manner, the emission spectrum will exhibit a fine structure. If the separation between impurities is greater than 40 Å, the emission lines will overlap, forming a broad spectrum. As

is evident from Eq (2), decreasing the impurity concentration results in a larger donor-acceptor separation and the emission energy shifts to a lower energy with a corresponding decrease in emission intensity (Ref 21:1000; 19:336-337). In undoped bulk grown GaAs, the broad band emission near 1.49 eV has been associated with distant donor-acceptor pair recombination.

The following characteristics of the 1.49 eV line are considered to be evidence for the donor-acceptor emission (Refs 19:336; 15:14).

1. A shift of the line to higher energies as the excitation intensity increases.

2. Appreciable narrowing of the emission band with an increase in intensity.

3. A shifting of the band toward higher energies as donor concentration increases.

4. A rapid decrease in intensity as the temperature increases from 25° K to 35° K.

5. A shift to higher energies as the temperature increases from 25° K to 35° K.

Phonon-Replicas. When the binding energy of an electron or a hole bound to a substitutional impurity increases, the interaction of the electron with the lattice gets stronger. These electron-lattice vibrations or phonon couplings result in the appearance of phonon-replicas in the emission spectra.

Two types of phonon replicas are possible: (i) longitudinal optical (LO) phonon replicas, and (ii) transverse acoustic (TA) phonon replicas.

In the emission spectra, when radiative transitions are phonon assisted, longitudinal optical phonons are separated in energy by 36 meV, whereas transverse acoustic phonons are separated by 9 meV.

As can be seen from Figure 4, for shallow simple centers such as zinc or cadmium, the phonon coupling is weak and only one LO phonon replica exists. For the deeper centers, such as copper and manganese, the phonon coupling is much stronger and two or three LO phonon replicas exist (Ref 19:388; 13:7-8).
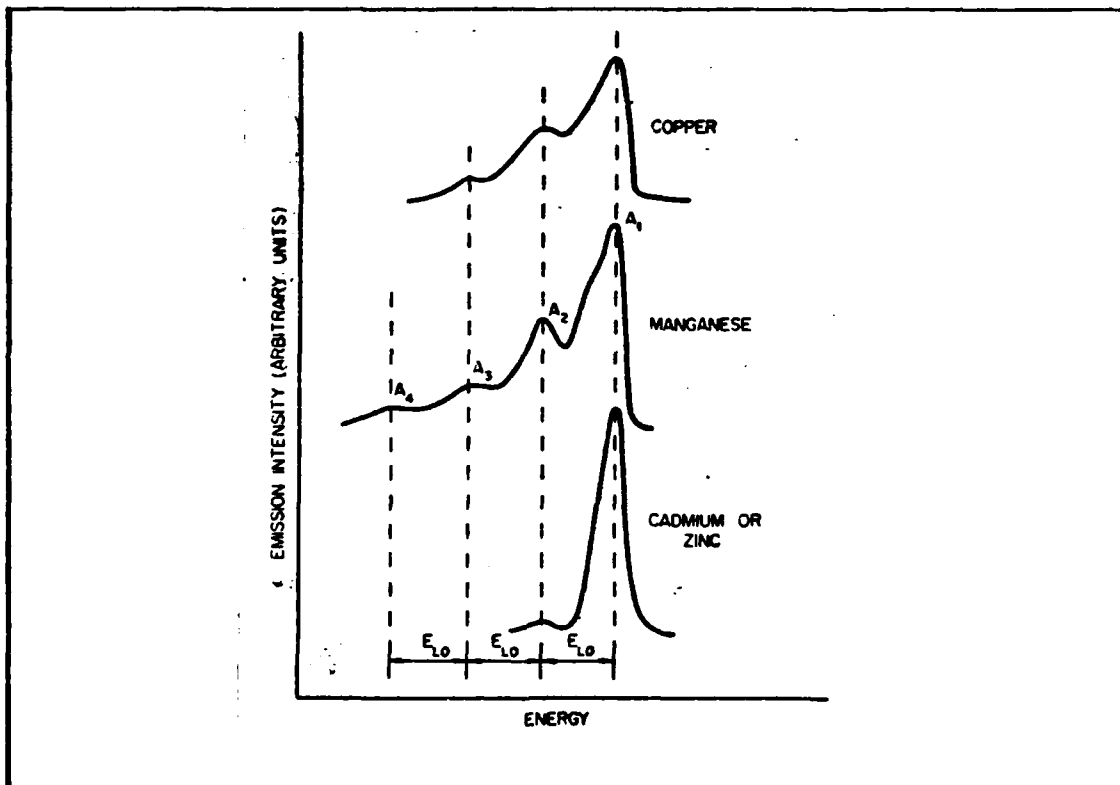
Figure 4. Phonon Emission of GaAs Doped with
Cadmium or Zinc, Manganese and Copper

19

Non-Radiative Recombination Processes

Unlike radiative recombination, which results in the emission of a photon, non-radiative recombination cannot be observed since this process does not result in the emission of a photon. The mechanisms for non-radiative recombination can only be deduced from such measurable parameters as emission efficiency and carrier lifetime (Ref 16:160). The following non-radiative processes are possible: (i) Auger effect, (ii) surface recombination, and (iii) multiple-phonon emission. Since these processes are purely non-radiative, and therefore cannot be observed during photoluminescence, they will briefly be discussed for the sole purpose of presenting a complete description of recombination processes in semiconductors.

Auger Effect. The Auger effect occurs when the energy released by an electron recombining with a hole is absorbed by another electron and this electron, in turn, dissipates the absorbed energy by interacting with the crystal lattice (phonon-coupling). Many Auger effects are possible, depending on the nature of the transitions and on the carrier concentration (Ref 16:161). Since the Auger effect is a carrier-carrier interaction process, the Auger effect will become more intense as the carrier concentration increases (Ref 16: 162).

20

Surface Recombination. Defects occurring near the surface will attract carriers that are within one diffusion length from the edge of the defect and non-radiative recombination by phonon emission will take place. As the carriers are depleted, the centers are continuously replenished by the diffusion process (Refs 22:7; 16:164-165).

Multiple-Phonon Emission. In multiple-phonon emission, a cascade of phonons is emitted during a non-radiative transition. Multiple-phonons are generated because the energy of the phonon is smaller than the energy released during recombination (Ref 16:167).

21

III. Equipment and Procedures

This chapter contains a description of the equipment used and experimental procedures utilized. It consists of five sections: sample preparation, sample environment, illumination source and optics, signal processing and experimental procedures.

Sample Preparation

Two semi-insulating GaAs:Cr wafers, manufactured by Crystal Specialties, Inc. (labeled E647-B-1 and E647-B-18), were provided by AFWAL/AADR. These wafers were different cuts from the ingot grown by the Horizontal Bridgman technique. Each wafer was cut to yield approximately 30 samples, each sample being 5 mm x 5 mm in size. Each sample was cleaned using established procedures.

Each sample was first scrubbed with basic H detergent, rinsed in deionized water and dried with nitrogen (N_2) gas. The samples were then rinsed with trichloroethylene, acetone and methanol. This action was a continuous process so as to keep the sample constantly wet. The samples were then rinsed again and blown dry with N_2 gas. After cleaning, the samples were etched in a 3:1:1 solution of $H_2SO_4:H_2O_2:H_2O$.

The purpose of this etch was to remove the damage surface layer that results from the polishing of the wafer by the manufacturer. The samples were then rinsed, blown dry

22

and then soaked in hydrochloric acid for oxide removal. A dark field microscope was used to visually inspect each sample. Those samples that showed excessive surface imperfections were eliminated. Each sample was then ready for capping to prevent the evaporation of As during the annealing process.

The samples were capped using plasma deposited Si_3N_4 at 325° C. The deposition layers varied from $\sim$500 Å to $\sim$1000 Å. After capping, each sample was visually inspected to ensure that no holes had formed in the cap.

Each sample was furnace annealed in flowing hydrogen (H_2) gas at temperatures ranging from 650° C to 950° C. One unannealed sample was retained from each wafer. A summary of the sample preparation is given in Table III.

After furnace annealing, the plasma caps were removed by submerging the samples in hydrofluoric acid for approximately ten minutes.

Van der Pauw measurements were made to determine which samples had thermally converted. Those samples that exhibited n-type thermal conversion were then subjected to profiling measurements to determine the depth of the converted layer. The results of the Van der Pauw and profiling measurements are discussed in Chapter IV.

Sample Environment

The sample environment is depicted in Figure 5. Two samples were mounted on a sample rod which was then inserted

	TABLE III	
	Summary of Sample Preparation	
Sample	Capped & Furance Annealed, 15 Min	Temp C
E647-B-18	2 each	650
"	"	700
"	"	750
"	"	800
"	4	850
E647-B-1	4	900
"	4	950

into a research dewar (Janis, Model DT). This dewar consisted of inner and outer reservoirs. During the experiment, the outer dewar was filled to capacity with liquid nitrogen (LN_2). The inner reservior was filled to capacity with liquid helium (LHe). Both reservoirs were surrounded by vacuum walls which were evacuated by a mechanical vacuum pump (Welch Scientific Co., Model 1397) and a diffusion pump (Consolidated Vacuum, Model PMC-115). Both pumps were operated continuously through-
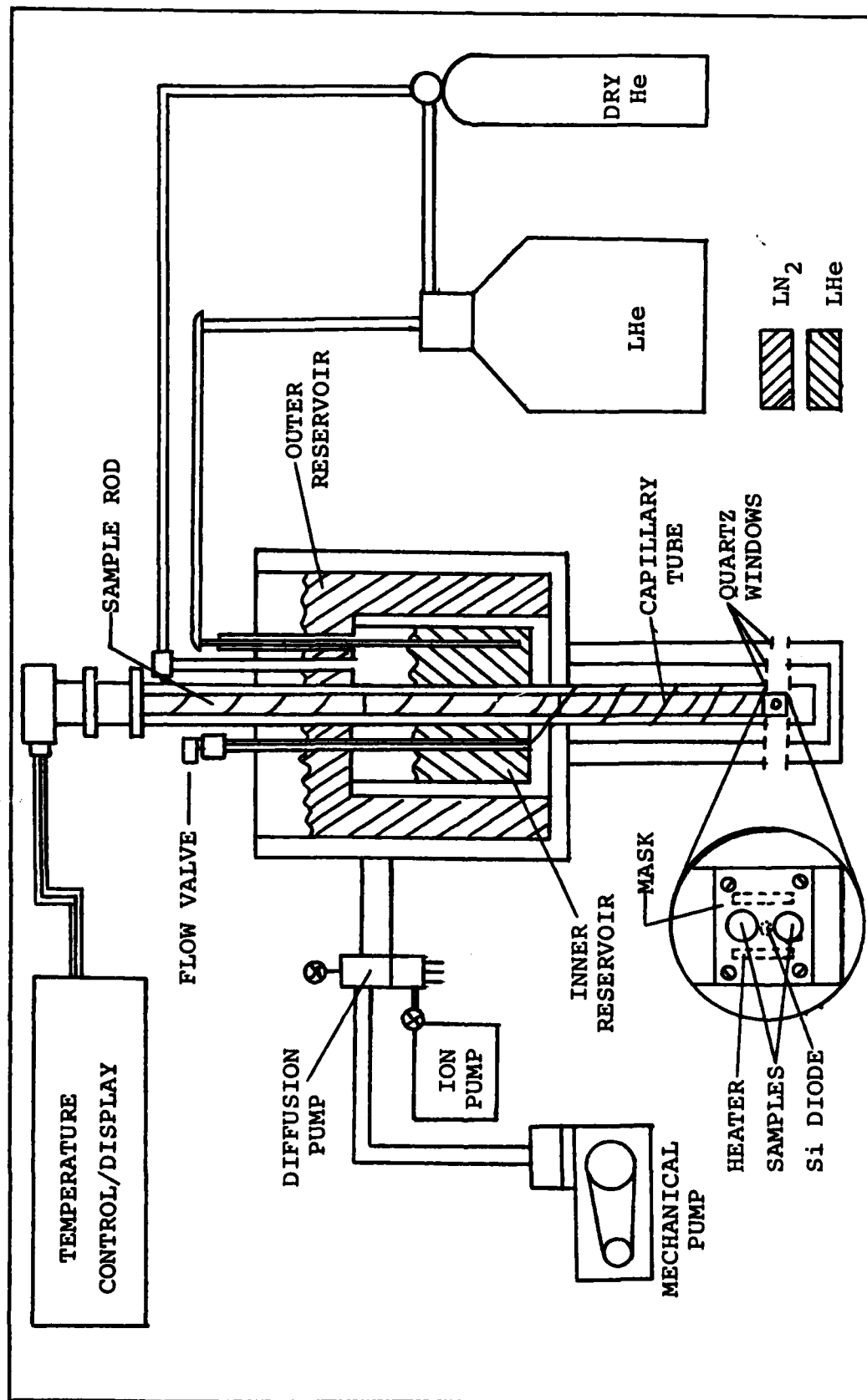
Figure 5. Sample Environment (Ref 15:21)

out the experiment. The samples were cooled by allowing LHe
to enter the sample chamber. The flow rate of LHe into the
sample chamber, and hence the cooling rate, was controlled
by operating a flow valve positioned at the top of the dewar.
The sample temperature was monitored by a temperature control-
ler unit (Lakeshore Cryotronics, Model DRC-80C).

Illumination Source and Optics

The diagram of the experimental setup is shown in
Figure 6. The samples were excited by a Coherent CR-500k
krypton laser. This laser produced ultraviolet (UV) lines
at 356.4 nm, 350.7 nm and 337.5 nm with a peak power of 30
milliwatts (mW). According to Pomrenke (Ref 23:5), the
average absorption coefficient for this laser is 6.84×10^5
cm^{-1} corresponding to a penetration depth of 146 $\overset{o}{A}$ at the
$\frac{1}{e}$ point. The diameter of the beam at the $\frac{1}{e^2}$ points was
1.1 mm. The output beam of the laser was passed through
a 350 nm bandpass filter to eliminate undesirable emissions
from the laser. An attempt was made to expand the beam in
order to reduce the Gaussian nature of the beam and thus pro-
vide near uniform illumination of the sample. Due to the
low output power and strong absorption characteristics of
the beam expander, there was insufficient illumination for
sample excitation and, therefore, this idea was discarded.
Sample illumination varied between 10 mW to 15 mW. The
laser beam was directed onto the sample by a 100% reflecting
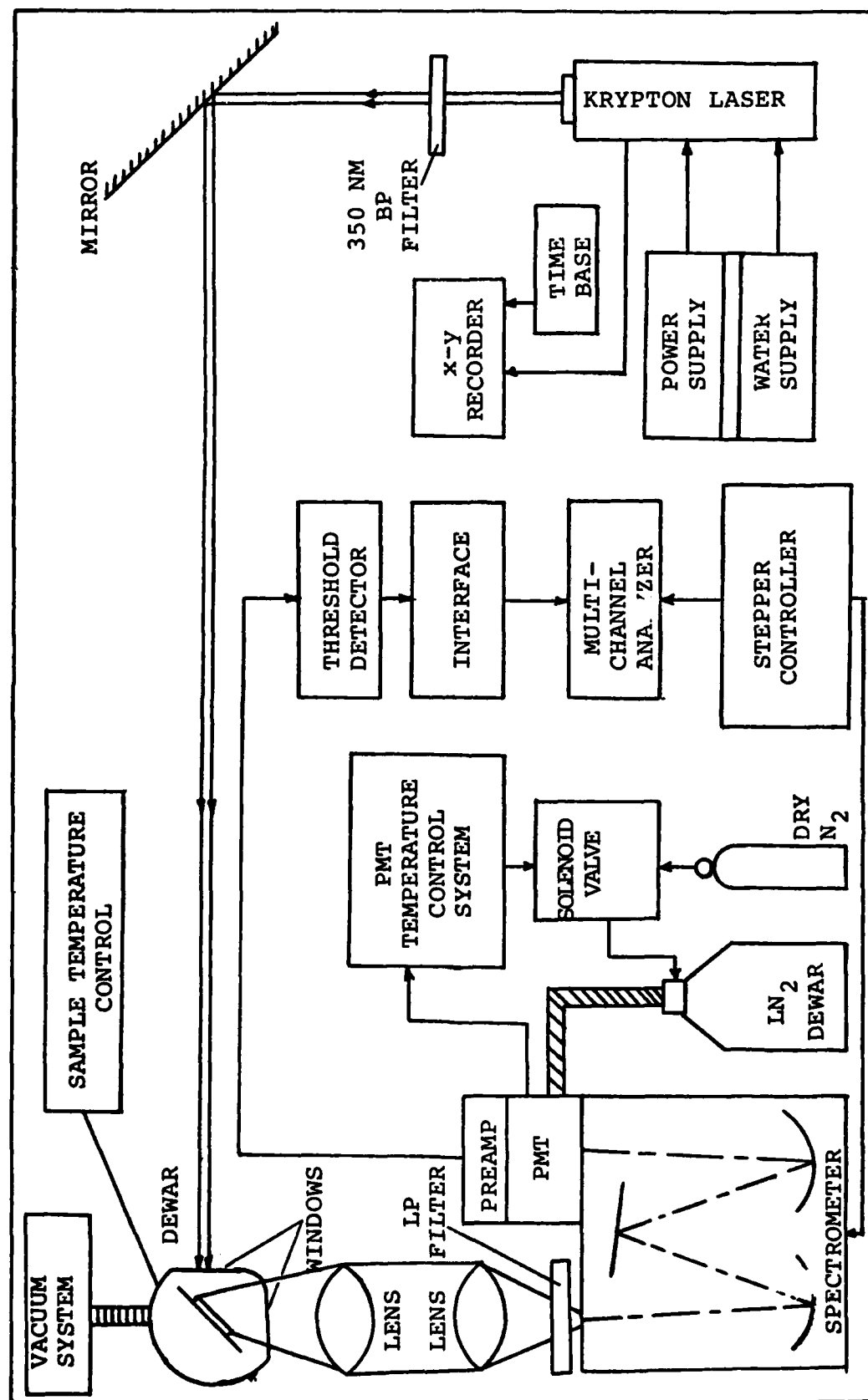UV mirror.

26

Figure 6. Photoluminescence System Diagram (Ref 15:24)

27

Photoluminescence emitted from the sample was collected and focused onto the spectrometer entrance slit by two bi-convex lenses. The first lens had a focal length of 100 mm and was placed one focal length away from the sample chamber. The second lens had a focal length of 200 mm and was placed one focal length from the entrance slit of the spectrometer. A 540 nm longpass filter was placed between the 200 mm lens and the entrance slit of the spectrometer to remove any undesirable emissions from the laser, as well as specular reflections from the sample, that would appear as higher order lines in the spectrum.

Signal Processing

The photoluminescence from the sample was dispersed by a Czerny-Turner 3/4 meter spectrometer (Spex, Model 1702). The grating in this spectrometer contained 1200 grooves/mm and was blazed at 5000 $\overset{\circ}{A}$. The scanning rate of the spectrometer was controlled externally by a motor stepper drive unit. All data were obtained at a scanning rate of 52.08 $\overset{\circ}{A}$/min. Slit widths of 0.5 mm and slit heights of 10 mm were used in all data runs.

A photomultiplier tube (PMT) (RCA, Model C70007A, S-1 type photocathode) housed in a refrigeration chamber (Prod-cuts for Research, Model TE-176-RF) was used to detect the photoluminescence. The PMT and refrigeration chamber were mounted at the exit slit of the spectrometer. The PMT was cooled to -50° C by pumping LN_2 into the refrigeration

28

chamber and the temperature was regulated by a temperature control unit (Products for Research, Model TE-176-RF). The bias voltage to the PMT was provided by a high voltage power supply (Princeton Applied Research, HVS-1). A bias voltage of 1350 V was applied to the PMT since this provided the optimum discrimination level between signal and noise.

The output from the PMT was connected to a threshold amplifier/discriminator unit (Princeton Applied Research, Model 1121). The output from the amplifier/discriminator unit was connected to an interface box which, in turn, provided the input signal to the multi-channel analyzer (MCA) (Hewlett Packard, Model 5400A). The MCA would take the number of counts coming from the amplifier/discriminator unit and store these counts in a particular address. The MCA would advance through 1024 channels and store counts in this manner. All data were taken with a MCA resolution of 1.732 $\overset{\circ}{A}$/channel. After all 1024 channels had been stepped through, a plot of counts versus wavelength could be displayed on the CRT of the MCA. This display was the resultant spectrum of the sample. The data could then be recorded onto paper tape for permanent storage and subsequent plotting.

Experimental Procedures

On the day before the measurement, two samples were mounted onto the sample rod and the rod was inserted into

29

the research dewar. On all data runs, one sample was used to gather data while the second was used to check the repeatability of the data. Reference marks on the top portion of the dewar ensured that the sample rod was con- sistently positioned at the same angle of incidence to the laser beam. The flow valve on the top portion of the dewar was opened, allowing helium gas to flow into the sample chamber, thus purging the chamber of any ambient air. During the purging, the outer reservoir of the dewar was slowly filled to capacity with LN_2. Once the outer reservoir had been filled, the flow valve was closed and the dewar was allowed to cool down overnight. To stabilize the PMT dark current, the bias voltage was applied to the PMT overnight. During all preparations, the entrance slit to the spectrometer was kept closed to preclude any excitation of the PMT from ambient light.

On the day of the experiment, the dewar was purged again with helium gas and filled to capacity with LN_2. Liquid helium was then transferred into the inner reser- voir. The flow valve, which controlled the flow of LHe into the sample chamber, was adjusted so that the sample temperature dropped at an even rate. During the period of sample cooldown, the laser was turned on and the PMT was cooled cryogenically to -50° C. This allowed ample time for the laser output power to stabilize and for the PMT dark cur- rent to be reduced. The sample to be studied was illumin- ated by a white light source and imaged onto the entrance

30

slit of the spectrometer by adjusting both biconvex lenses. The two lenses were adjusted so as to produce an image that overfilled the entrance slit with maximum illumination. After the optics had been aligned, all remaining devices were turned on and their switches set for the data run.

The lighting in the room was reduced to a minimum and the entrance slit to the spectrometer was opened. A black cloth was draped over the front window of the sample chamber to prevent any luminescence from reaching the spectrometer. On all data runs, the spectrometer wavelength meter was set at approximately 8000 $\overset{\circ}{A}$. After the sample temperature had stabilized at 5° K, an argon calibration lamp, placed near the entrance slit, was turned on. This would introduce two known lines at 8006.16 $\overset{\circ}{A}$ and 8014.79 $\overset{\circ}{A}$. Once the lamp was turned on, the spectrometer drive was begun, followed by the MCA. When the two known lines were detected, the argon lamp was turned off simultaneously with the removal of the black cloth from the sample chamber window.

During each data run, which lasted 34 minutes, the sample temperature and laser output power were monitored. After the data run was completed, the spectrum was examined and recorded onto paper tape. The paper tapes generated were subsequently converted to card format for the generation of the spectral plots which appear in this

31

thesis. Once the data was recorded, the second sample to be studied was placed in position by adjusting the research dewar up or down.

IV. Experimental Results

This chapter contains a discussion of the results of this thesis. Included in this chapter is a discussion of photoluminescence spectra obtained before and after annealing, as well as a discussion of changes in spectra obtained after removal of surface layers from the thermally converted samples. The spectral plots which appear in this chapter are plotted on the same scale with different vertical offsets. This type of representation allows for easier comparisons between individual spectra. In addition, "expanded views" are provided to show further detail of the spectra.

Photoluminescence of Unannealed Samples

Figures 7 and 8 show the spectra of unannealed SI GaAs:Cr samples. Both spectra show the presence of a peak at 1.5147 eV and 1.5144 eV, which is attributed to an exciton bound to a neutral donor (Si) (Refs 18:341-342; 21:995). The peaks at 1.4941 eV and 1.4957 eV are believed to be free-to-bound transitions due to carbon acceptors (C_{As}). The peak due to C_{As} has been reported at 1.4930 eV (Ref 12:4863) and 1.4935 eV (Ref 24:1051). The peaks at 1.4848 and 1.4851 are due to conduction band-to-bound acceptors due to Si (Ref 24:1051). The peaks at 1.4478 eV and 1.4505 eV are LO phonon replicas of the 1.4848 eV and 1.4851 eV peaks, respectively. In both figures, the slight peak at 1.4076 eV is attributed to an As vacancy to Si acceptor ($V_{As} - Si_{As}$) transition
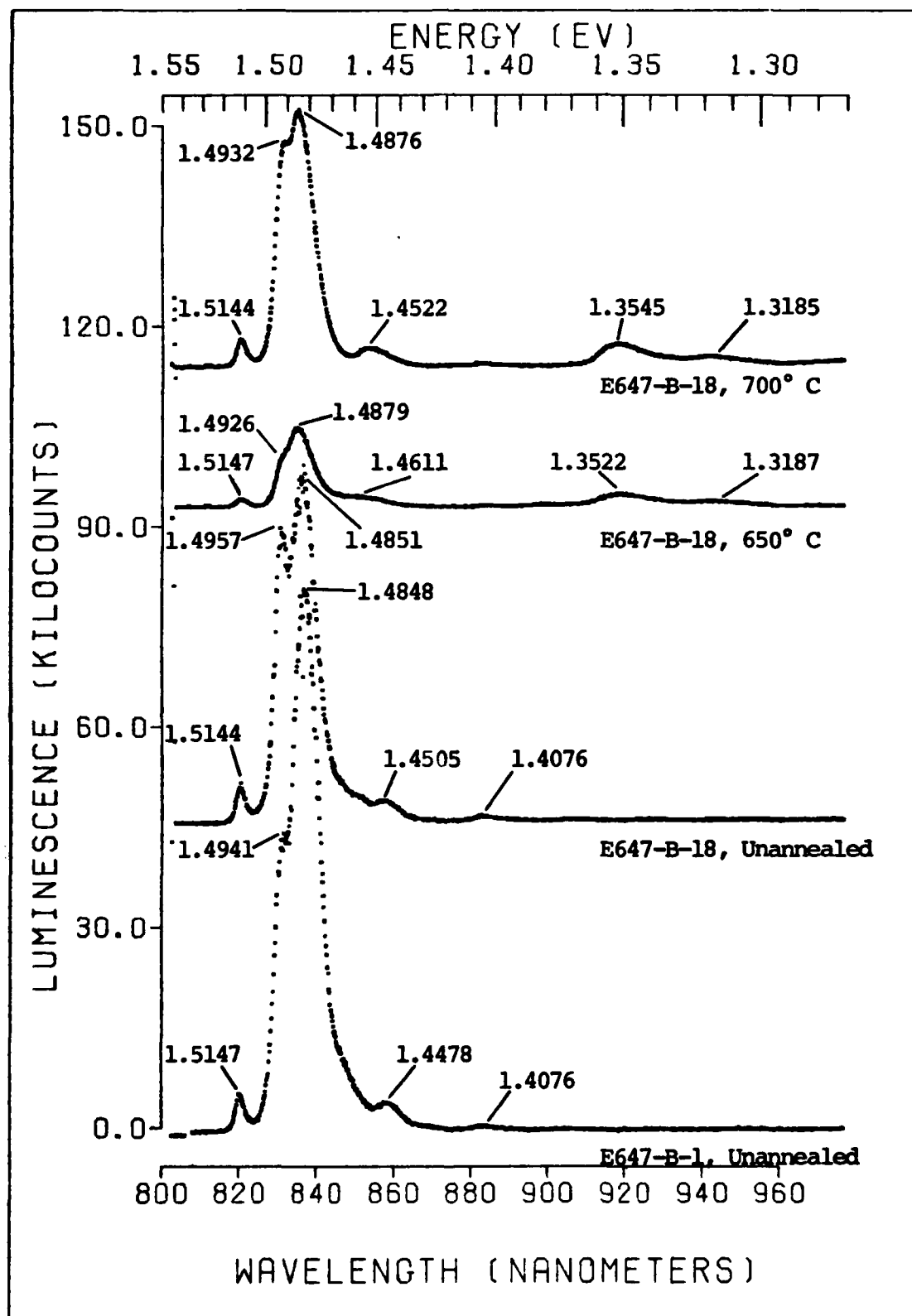
33

Figure 7. Photoluminescence of Unannealed Samples
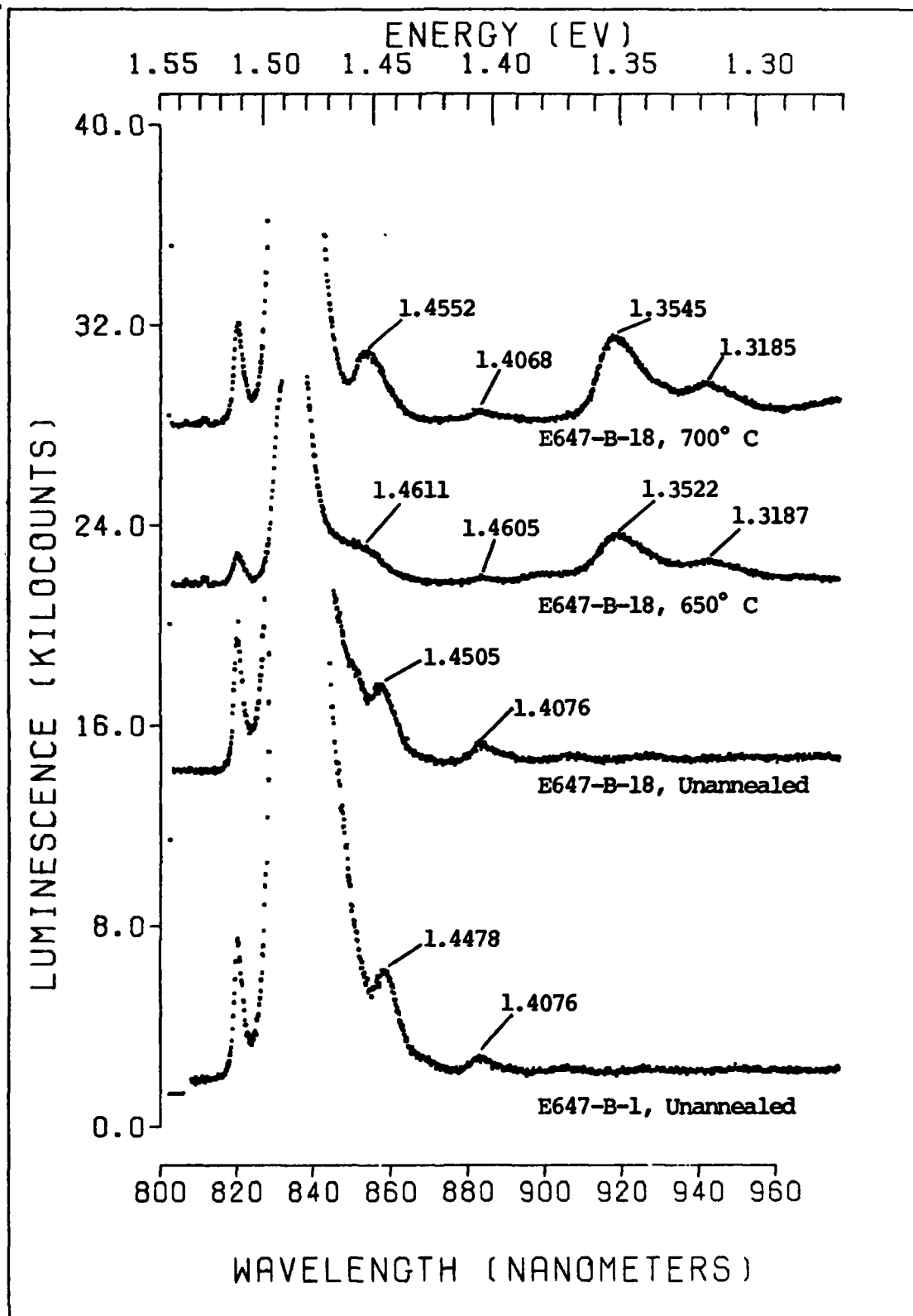and Samples Annealed at 650° C and 700° C

34

Figure 8. Expanded View of Figure 7

(Ref 15:37; 12:4811). This peak is commonly observed in uncapped samples that have been annealed at high temperatures due to the increased generation of As vacancies. However, it should be noted that this peak is present in all of the spectra but becomes more noticeable at the higher anneal temperatures.

The increase in As vacancies suggests that the Si_3N_4 caps do not prevent the escape of arsenic during the annealing process.

Photoluminescence of Annealed Samples

Figures 7 and 8 also show the photoluminescence of samples annealed at 650° C and 700° C. The peaks located at 1.4879 eV and 1.4876 eV, respectively, are identified as conduction band-to-bound zinc acceptor transitions (Ref 24:1051). For the sample annealed at 650° C, an unresolved peak appears at approximately 1.4611 eV which may be a LO phonon replica of the main peak. The separation in energy from the main peak is 26 meV, which is less than what is defined for a LO phonon replica. The exciton transition for this sample is located at 1.5147 eV. The carbon acceptor transition (1.4926 eV) appears as a shoulder on the high energy side of the main peak and the silicon acceptor peak has disappeared. In the sample annealed at 700° C, the C_{As} transition is clearly discernible at 1.4932 eV. Again, the Si_{As} peak is not present. The LO phonon replica of the

main peak appears at 1.4552 eV, whereas the exciton transition lies at 1.5144 eV. Both samples exhibit the conduction band-to-copper acceptor transition (Cu_{Ga}) at 1.3522 eV and 1.3545 eV, respectively. This transition has been reported at 1.356 eV (Ref 25:5340) and at 1.359 eV (Ref 12:4863). The peaks at 1.3188 eV and at 1.3185 eV are the LO phonon replicas of the Cu_{Ga} transition. Note that the Cu_{Ga} peak has begun to increase. The V_{As}-Si_{As} peak is present in both samples at 1.4065 eV and 1.4068 eV, respectively.

Figures 9 and 10 show the photoluminescence spectra for samples annealed at 750° C and 800° C. From Figure 9, it can be seen that the luminescence from the sample annealed at 750° C is much greater than what has been previously observed. The zinc acceptor transition (1.4882 eV) is very strong, whereas the C_{As} peak (1.4944 eV) is approximately four times greater than in the sample annealed at 700 C. The LO phonon replicas of these peaks are located at 1.4576 eV and 1.4519 eV, respectively. Note that the V_{As}-Si_{As} peak (1.4084 eV) has begun to increase and the Cu_{Ga} acceptor peak (1.3576 eV) is beginning to decrease. The exciton transition is located at 1.5147 eV. In the sample annealed at 800° C, the carbon acceptor peak (1.4931 eV) appears as a slight shoulder on the high energy side of the main peak. The zinc acceptor peak remains the dominant peak at 1.4873 eV. The LO phonon replica for this
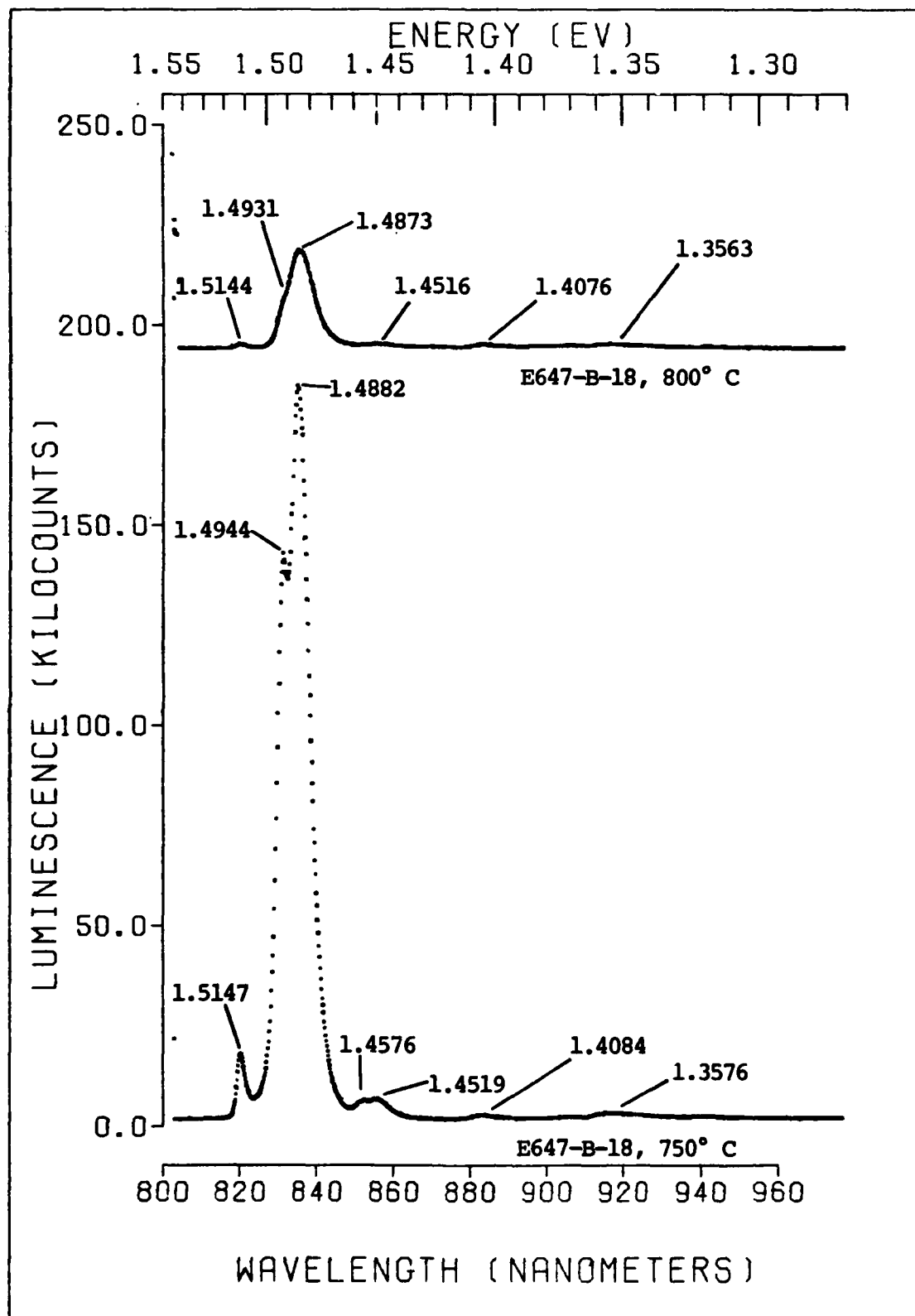
37

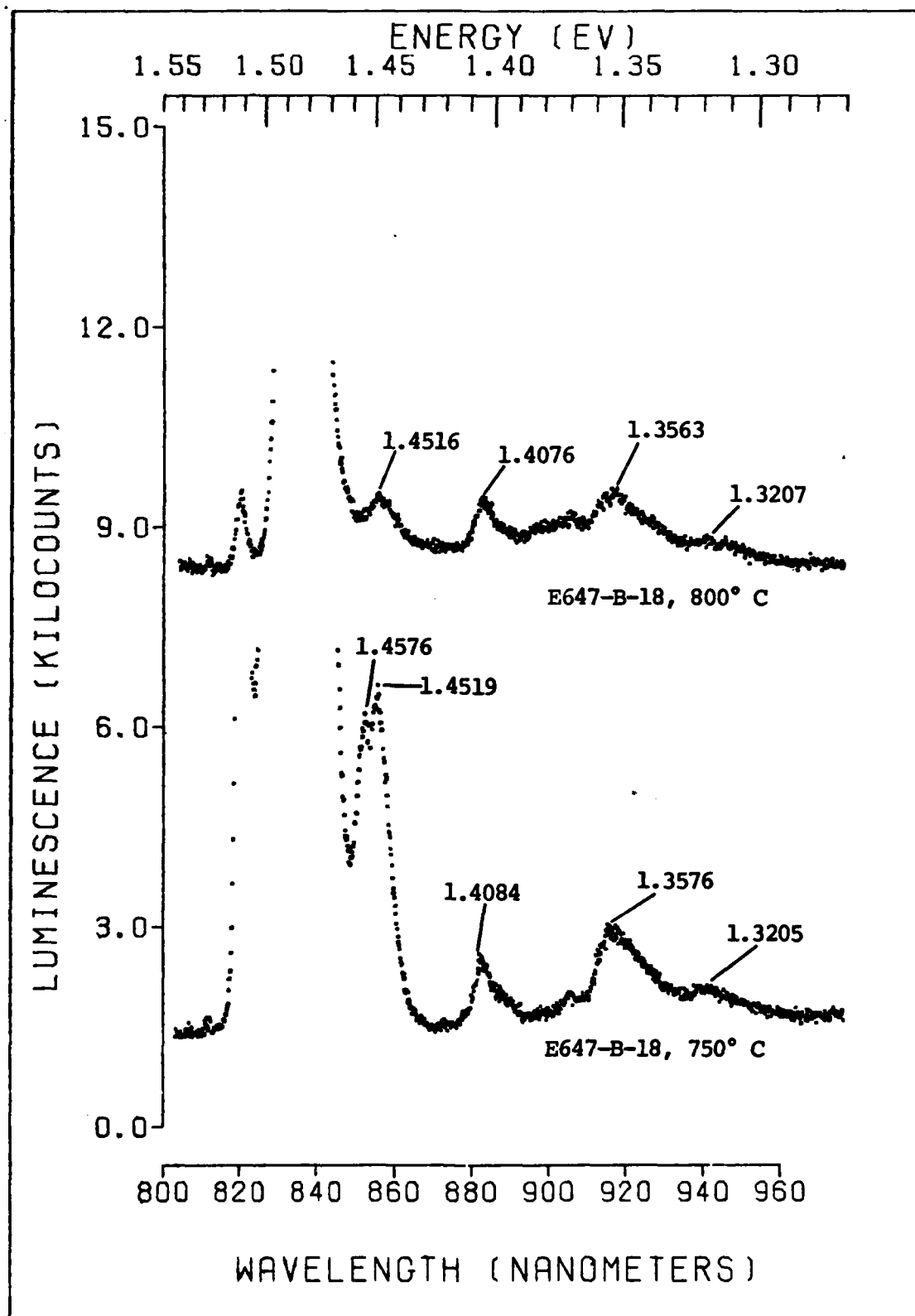Figure 9. Photoluminescence of Samples Annealed at 750° C and 800° C

38

Figure 10.   Expanded View of Figure 9

peak appears at 1.4516 eV. The V_{As}-Si_{As} peak (1.4076 eV) continues to increase, whereas the Cu_{Ga} peak (1.3563 eV) continues to decrease.

In Figures 11 and 12, the photoluminescence spectra begin to show a change from previous spectra. The spectrum of the sample annealed at 850° C shows the zinc acceptor peak (1.4879 eV) to be the dominant peak with its LO phonon replica located at 1.4525 eV. The Si acceptor peak (1.4848 eV) reappears as a slight shoulder on the low energy side of the main peak. The carbon acceptor peak (1.4922 eV) is evident as a slight shoulder, but on the high energy side of the main peak. The phonon replicas of these peaks are located at 1.4555 eV and 1.4493 eV, respectively. The V_{As}-Si_{As} peak (1.4073 eV) is approximately four times greater than at the previous anneal temperature and its associated TA and LO phonon replicas begin to emerge. The TA phonon replicas are located at 1.3997 eV and 1.3602 eV, whereas the LO phonon replicas are located at 1.3714 eV and 1.3244 eV. These series of peaks have also been observed by other researchers (Ref 2: 227-223; 9:232). For the sample annealed at 900° C, the exciton peak has shifted to a higher energy (1.51598 eV) which is believed to be due to an exciton bound to a donor other than Si. The Zn_{Ga} peak is present as a shoulder at 1.490 eV, along with the C_{As} peak at 1.4941 eV. The Si_{As} peak (1.4860 eV) has become the dominant peak. The phonon
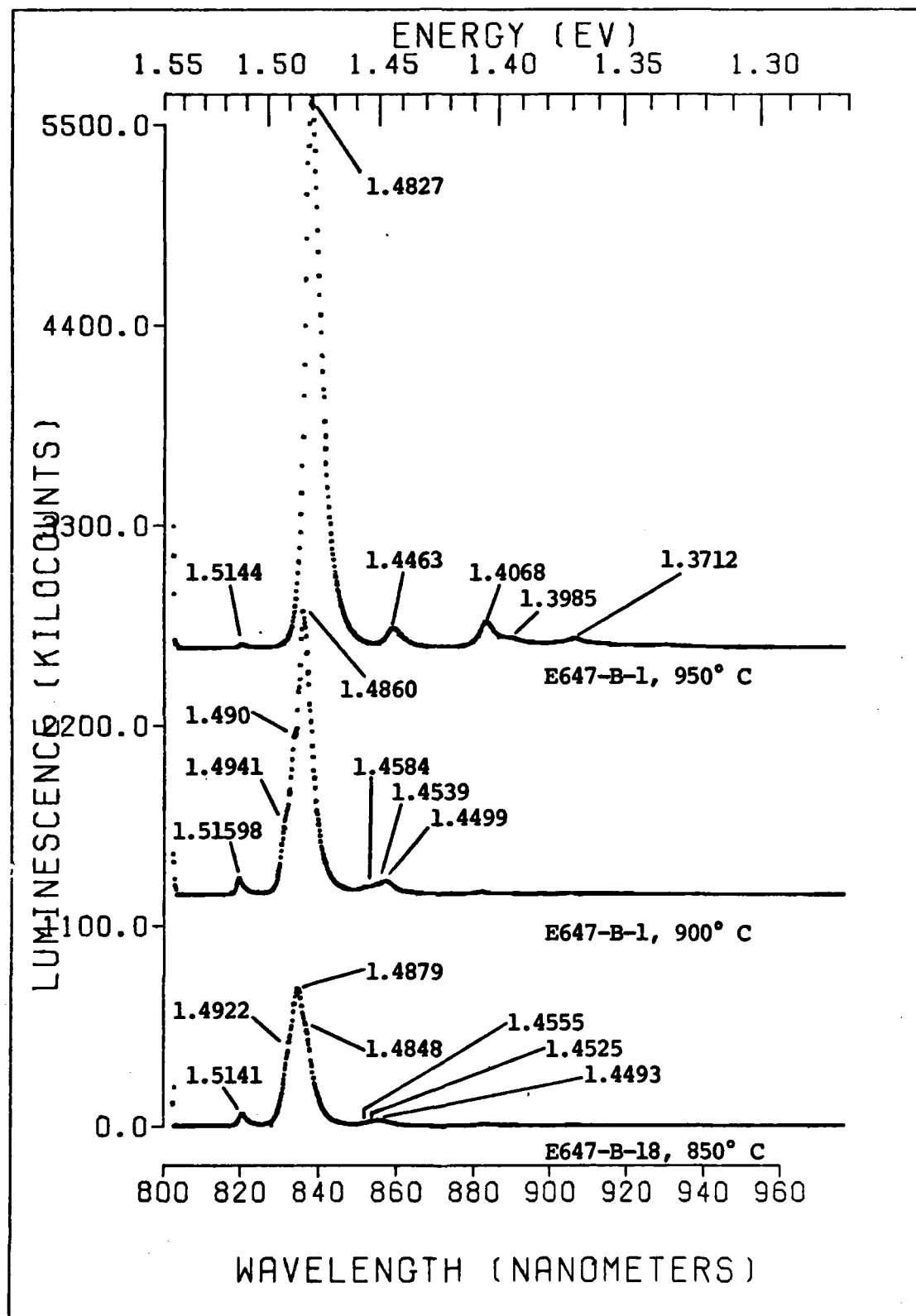
Figure 11. Photoluminescence of Samples Annealed
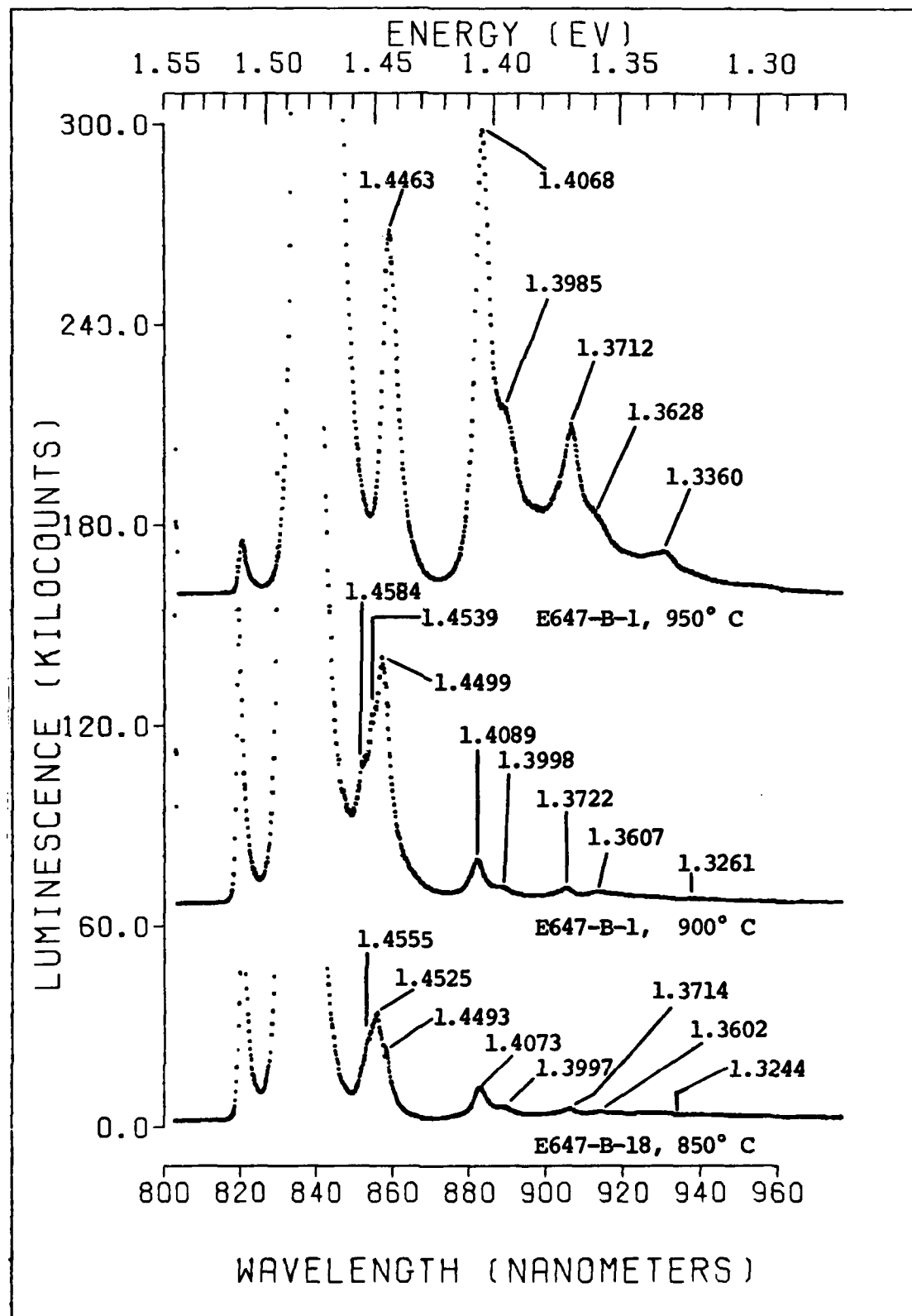at 850° C, 900° C, and 950° C

41

Figure 12. Expanded View of Figure 11

replicas of the carbon, zinc and silicon peaks are at 1.4584 eV, 1.4539 eV and 1.4499 eV. The V_{As}-Si_{As} peak appears at 1.4089 eV, along with its TA and LO phonon replicas at 1.3998 eV, 1.3722 eV, 1.3607 eV and 1.3261 eV. There is an increase in the intensity of the V_{As}-Si_{As} peak suggesting that As vacancy generation is increasing. For the sample annealed at 950° C, the amplitude of the V_{As}-Si_{As} complex (1.4068 eV) is eleven times greater than at the previous anneal temperature. Clearly, this is due to the larger number of As vacancies created at this temperature. An unknown peak appears as the dominant peak at 1.4827 eV, along with its associated LO phonon replica at 1.4463 eV. It is not known what acceptor impurity is responsible for this peak, nor is it known what role, if any, this peak has in thermal conversion. Note that, for these sets of samples, the 1.35 eV peak associated with copper acceptor transitions has disappeared or is lost under the As vacancy peaks. The TA and LO phonon replicas of the As vacancy peak (1.4068 eV) are located at 1.3985 eV, 1.3712 eV, 1.3628 eV and 1.3360 eV.

Results of Van der Pauw Hall Measurement

Van der Pauw Hall measurements were conducted at AFWAL/AADR to determine which samples exhibited n-type conversion. A brief description of this procedure follows.

Indium contacts were soldered to the corners of the samples with a vibrational soldering iron and then the samples were annealed at 350° C for three minutes to remove any effects from this procedure. The samples were then tested for good ohmic behavior prior to performing the Hall measurements. Those samples that exhibited a linear I-V characteristic were then subjected to Hall measurements to determine the surface type. These results are shown in Table 4. As can be seen from Table 4, all samples annealed at 900° C and 950° C thermally converted. Of the four samples annealed at 850° C, one converted, one showed mixed conductivity, and two did not convert.

Resistivity Profile Measurements

Those samples which exhibited n-type thermal conversion were subjected to electrical profile measurements to determine the extent of the converted surface layer. The procedures used in preparing the samples for resistivity measurements were the same as described in the section on Van der Pauw Hall measurements. Resistivity measurements were recorded at various etch depths. The etch solution used was a 1:1:50 solution of $H_2O_2:H_2SO_4:H_2O$ at room temperature. Although the etch solution was calibrated at 1200 Å/min by a Sloan Detak surface profiling instrument, the actual etch rate measured was 564 and 594 Angstroms per minute. It is speculated that differences between the calibration solution and etching

44

TABLE 4

Results of Van der Pauw Hall Measurements

Sample	Anneal Temperature ° C	Surface Type	Resistivity (ohms)
E647-B-18	650	SI	---
"	700	SI	---
"	750	SI	---
"	800	SI	---
"	850	N	4.65×10^5
E647-B-1	900	N	7.65×10^3
"	950	N	1.22×10^3

solution, resulting from the shelf life of the chemicals, was responsible for the difference in etching rates.

Tables 5 and 6 show the results of the resistivity profile measurements for the samples annealed at 900° C and 950° C, respectively. Resistivity profile measurements were not made for the sample annealed at 850° C. For the

TABLE 5

Resistivity Profile Measurement

for Sample E647-B-1 Annealed at 900° C

Average Etch Depth ($\overset{\circ}{A}$)	Resistivity (ohms)	Surface Type
0	7.65×10^3	N
496.39	7.83×10^3	N
744.59	9.899×10^3	N
992.78	1.85×10^4	N
1489.17	4.00×10^5	M*
2035.199	5.53×10^5	M*

*M = Mixed Conductivity

sample annealed at 900° C, the depth of the converted layer is between 992.78 $\overset{\circ}{A}$ and 1489.17 $\overset{\circ}{A}$. For the sample annealed at 950° C, the converted layer is between 4691.00 $\overset{\circ}{A}$ and 6801.95 $\overset{\circ}{A}$.

46

TABLE 6

Resistivity Profile Measurement

for Sample E647-B-1 Annealed at 950° C

Average Etch Depth ($\overset{\circ}{A}$)	Resistivity (ohms)	Surface Type
0	1.22×10^3	N
234.55	$1.23 \ c \ 10^3$	N
469.10	$1.19 \ c \ 10^3$	N
703.65	1.22×10^3	N
938.20	1.26×10^3	N
1172.75	1.31×10^3	N
1407.30	1.21×10^3	N
1876.40	1.49×10^3	N
2345.50	1.65×10^3	N
3283.70	2.29×10^3	N
4691.00	5.73×10^3	N
6801.95	4.95×10^4	M
7740.15	8.29×10^4	M
9382.00	8.43×10^4	M

*M = Mixed Conductivity

Depth Resolved Photoluminescence

Figures 13 through 18 show the depth resolved photo-luminescence spectra for samples annealed at 850° C, 900° C and 950° C. The purpose in performing these measurements was to record changes in the spectra of the thermally converted samples as surface layers were removed.

In Figure 13, the carbon acceptor peak (1.4954 eV) is clearly visible at an etch depth of 8797 Å. In actuality, this peak becomes visible at an etch depth of 3258 Å, but this spectrum was not available for publication. The zinc acceptor peak (1.4879 eV) continues to be the dominant peak. The LO phonon replicas of these peaks are at 1.4582 eV and 1.4522 eV, respectively.

At an etch depth of 1.6 μm, the silicon acceptor peak (Si_{As}) appears as a shoulder at approximately 1.4848 eV. The Zn_{Ga} peak continues to remain as the dominant peak at 1.4867 eV. The C_{As} peak appears at 1.4960 eV. The phonon replicas of the C_{As} and Zn_{Ga} peaks appear at 1.4587 eV and 1.4519, respectively. At an etch depth of 3.9 μm, the main peak is at a lower energy (1.4860 eV) than at the previous etch. However, it is speculated that the zinc acceptor peak is still the dominant peak at this etch depth. A slight shoulder appears on the low energy side of the main peak at approximately 1.4830 eV and is believed to be due to Si_{As}. The phonon replicas of the C_{As} (1.4953 eV) and Zn_{Ga} (1.4860 eV)
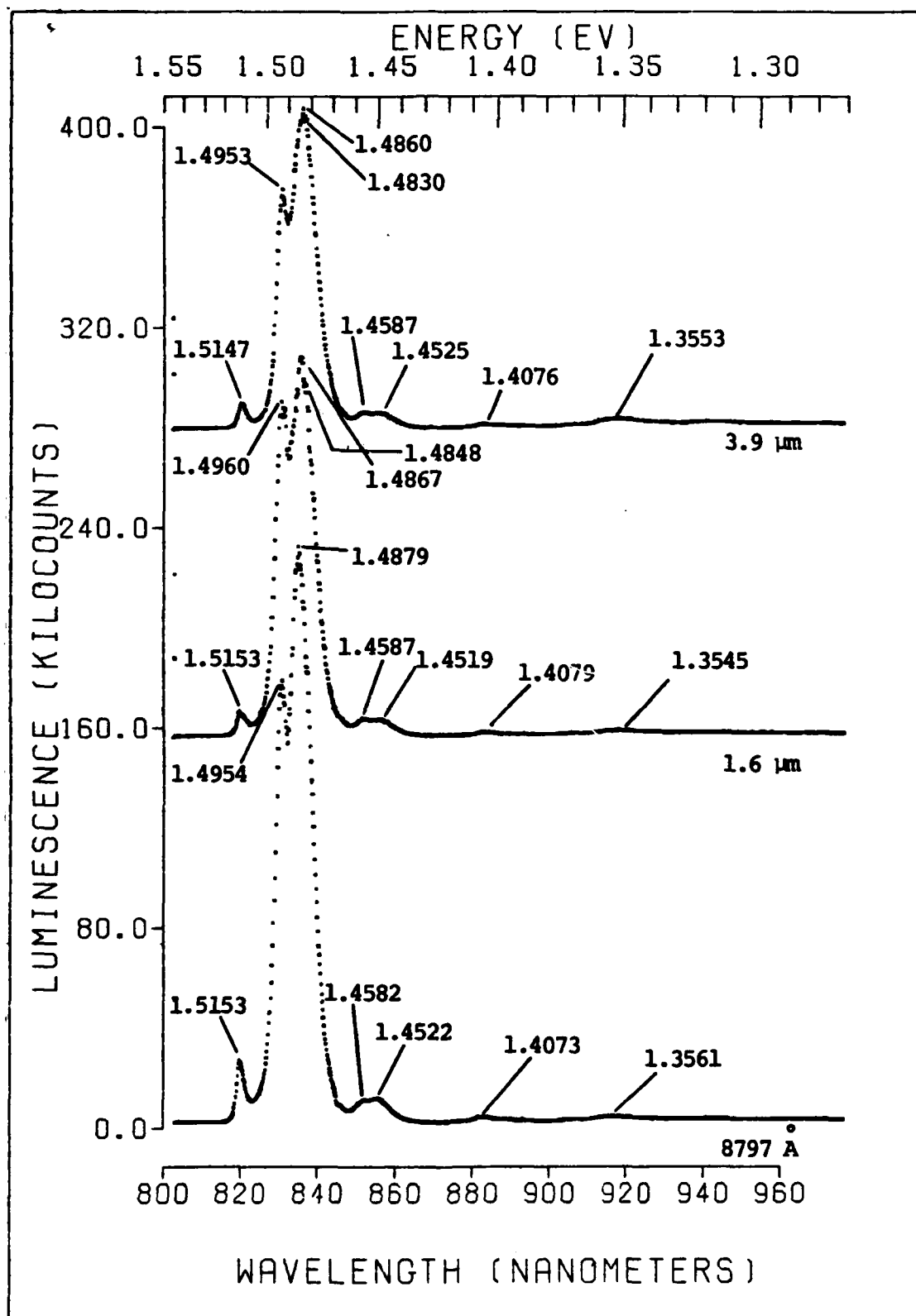
Figure 13. Depth Resolved Photoluminescence
of Sample Annealed at 850° C

49
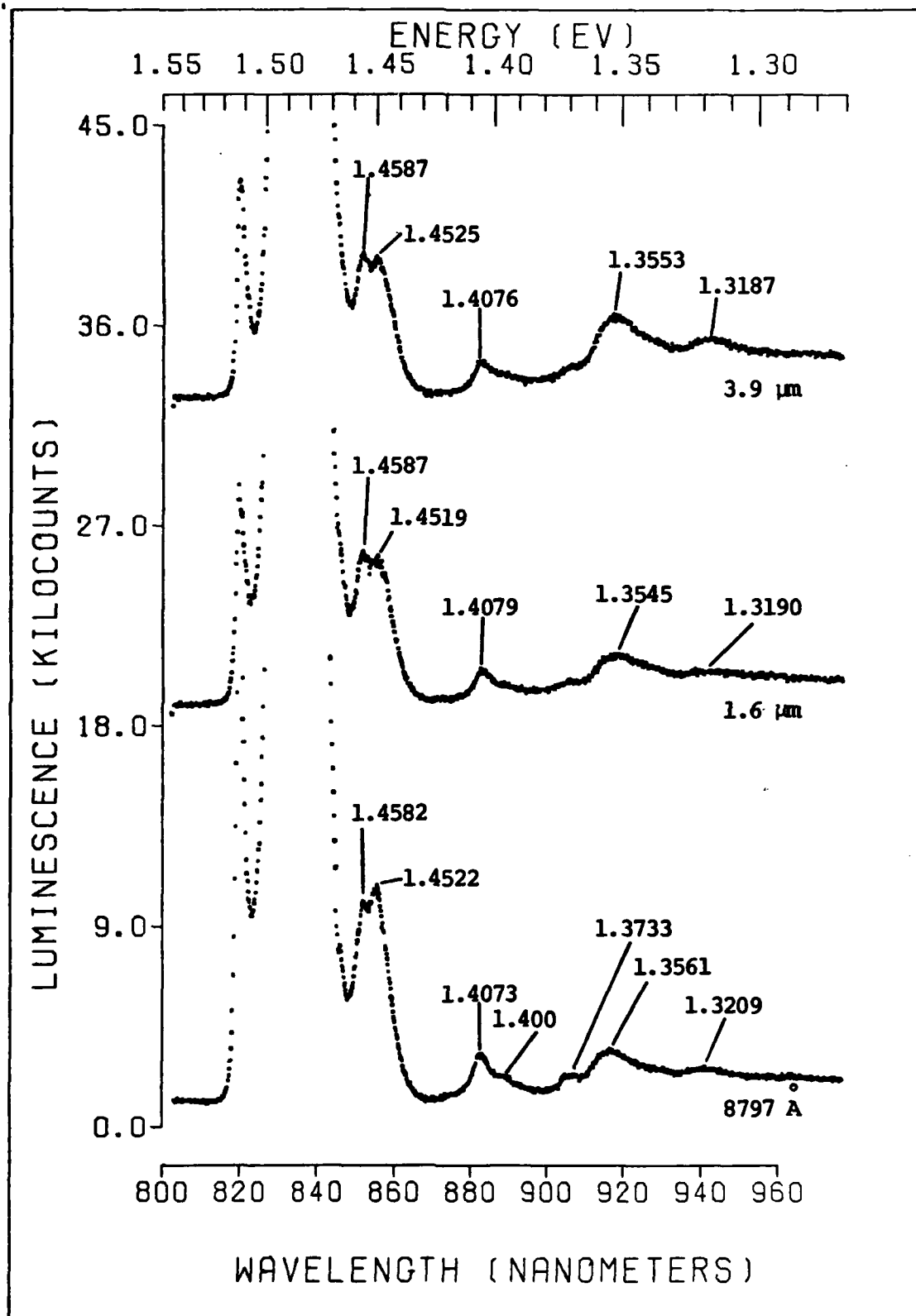
Figure 14.   Expanded View of Figure 13

peaks are located at 1.4587 eV and 1.4525 eV, respectively. Note that, throughout this series of etchings, the $(V_{As}-Si_{As})$ peak (1.407 eV) has decreased in intensity and its associated LO and TA phonon replicas have been replaced by the Cu_{Ga} peak (1.3553 eV) and its LO phonon replica (1.3187 eV). The depth resolved photoluminescence for the sample annealed at 900° C is shown in Figures 15 and 16.

Up until an etch depth of 1.5 μm, the dominant peak was due to silicon acceptors. At this etch depth, the Zn_{Ga} peak (1.4891 eV) became dominant. A possible explanation for this anomaly may be that the silicon and zinc impurities are inhomogeneously distributed throughout the material and that the peaks trade off as dominant peaks. The C_{As} peak (1.4932 eV) is present on the high energy side of the main peak as a shoulder. The phonon replicas of the C_{As} and Zn_{Ga} peaks appear at 1.4576 eV and 1.4531 eV, respectively. The $V_{As}-Si_{As}$ peak appears at 1.4084 eV along with its TA and LO phonon replicas at 1.3996 eV, 1.3722 eV, 1.3592 eV and 1.3246 eV. At an etch depth of 3.1 μm, the Zn_{Ga} (1.4879 eV) peak continues to be the dominant peak. The C_{As} peak is located at 1.4947 eV. In this case, only one LO phonon replica, associated with Zn_{Ga}, is visible at 1.4579 eV. At this etch depth, the Cu_{Ga} peak, along with its LO phonon replica are becoming visible at 1.3568 eV and 1.3222 eV. Note that the amplitude of the $V_{As}-Si_{As}$ peak (1.4082 eV) has decreased. When the sample is etched 7.5 μm,
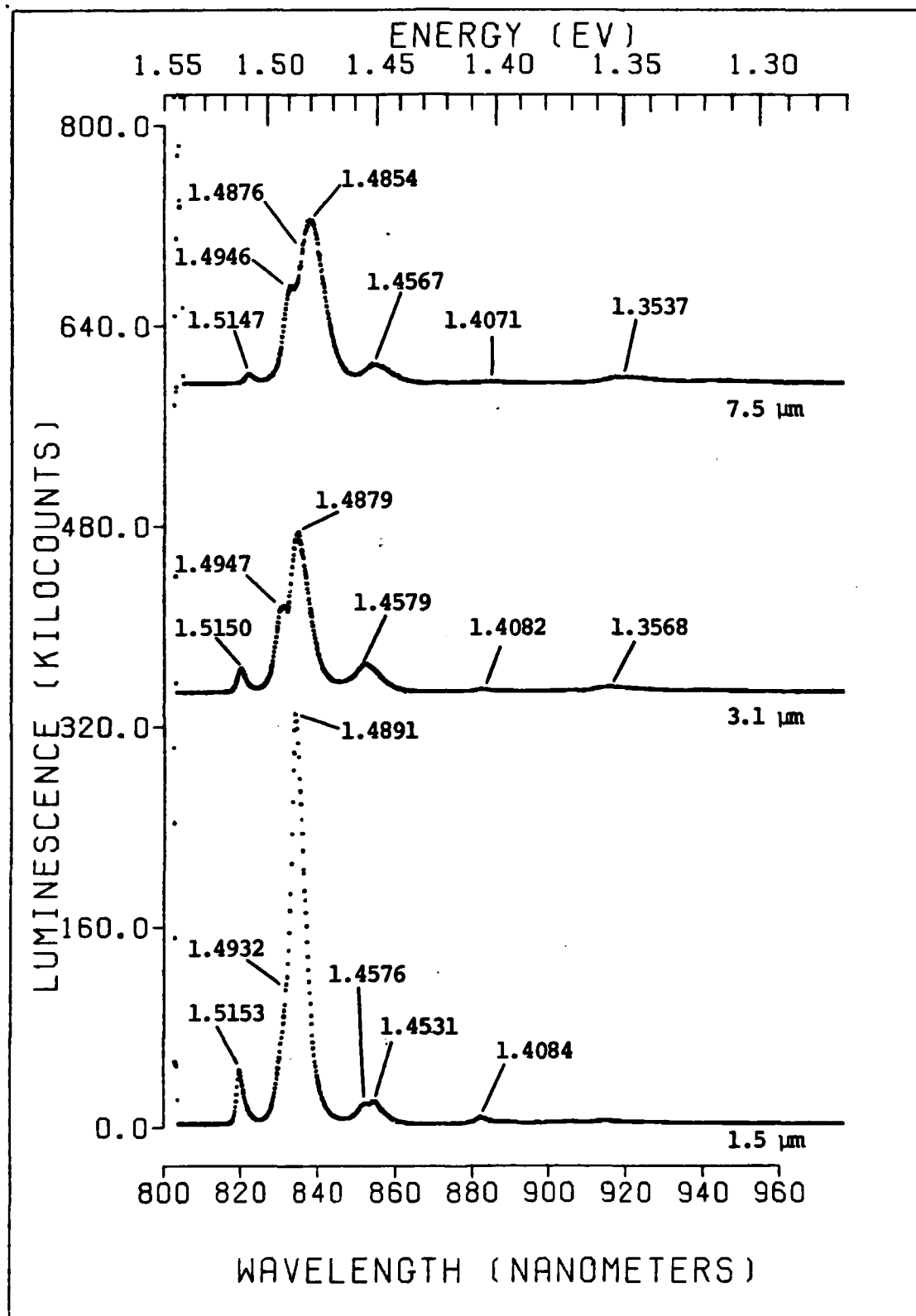
51

Figure 15. Depth Resolved Photoluminescence
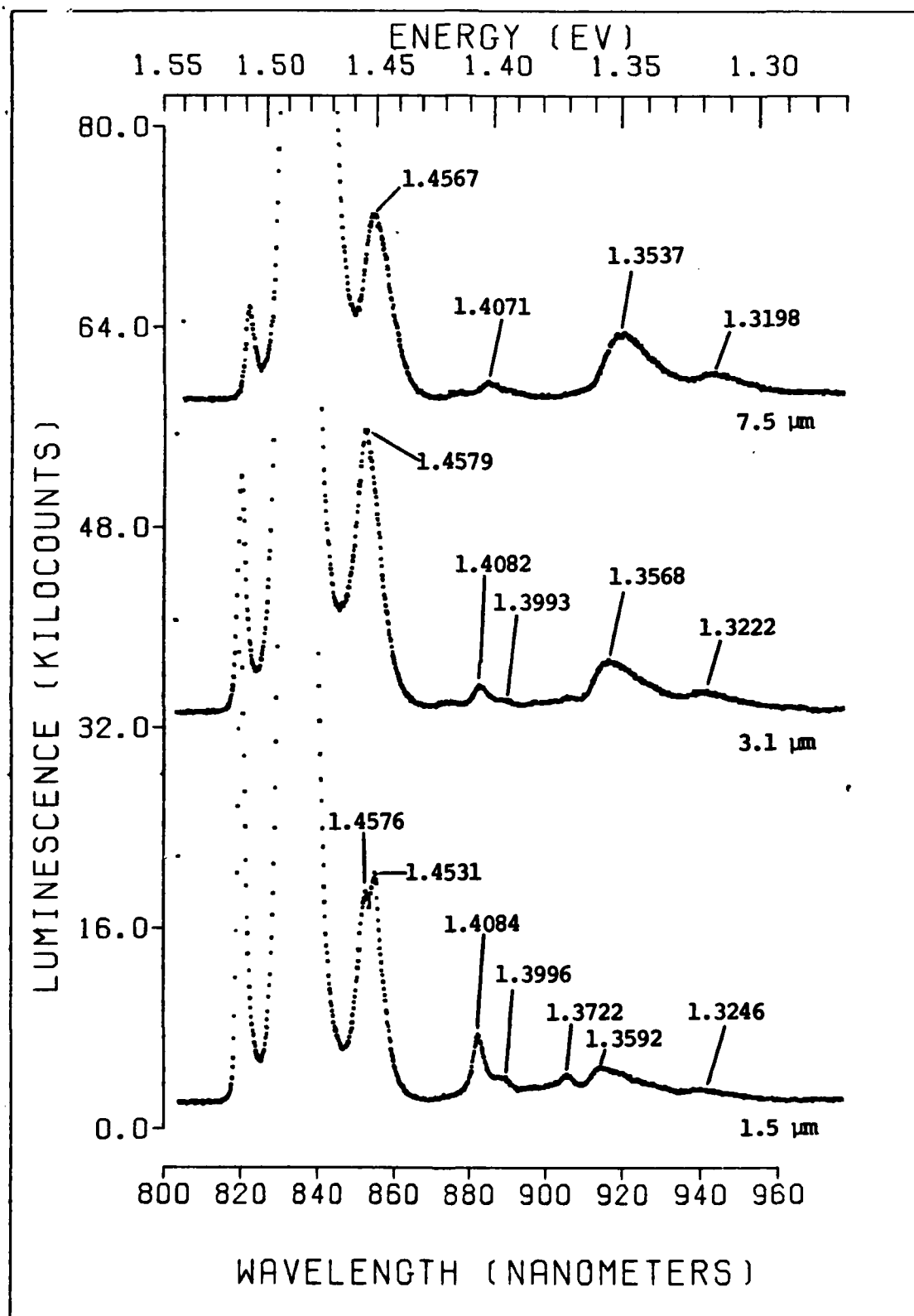of Sample Annealed at 900° C
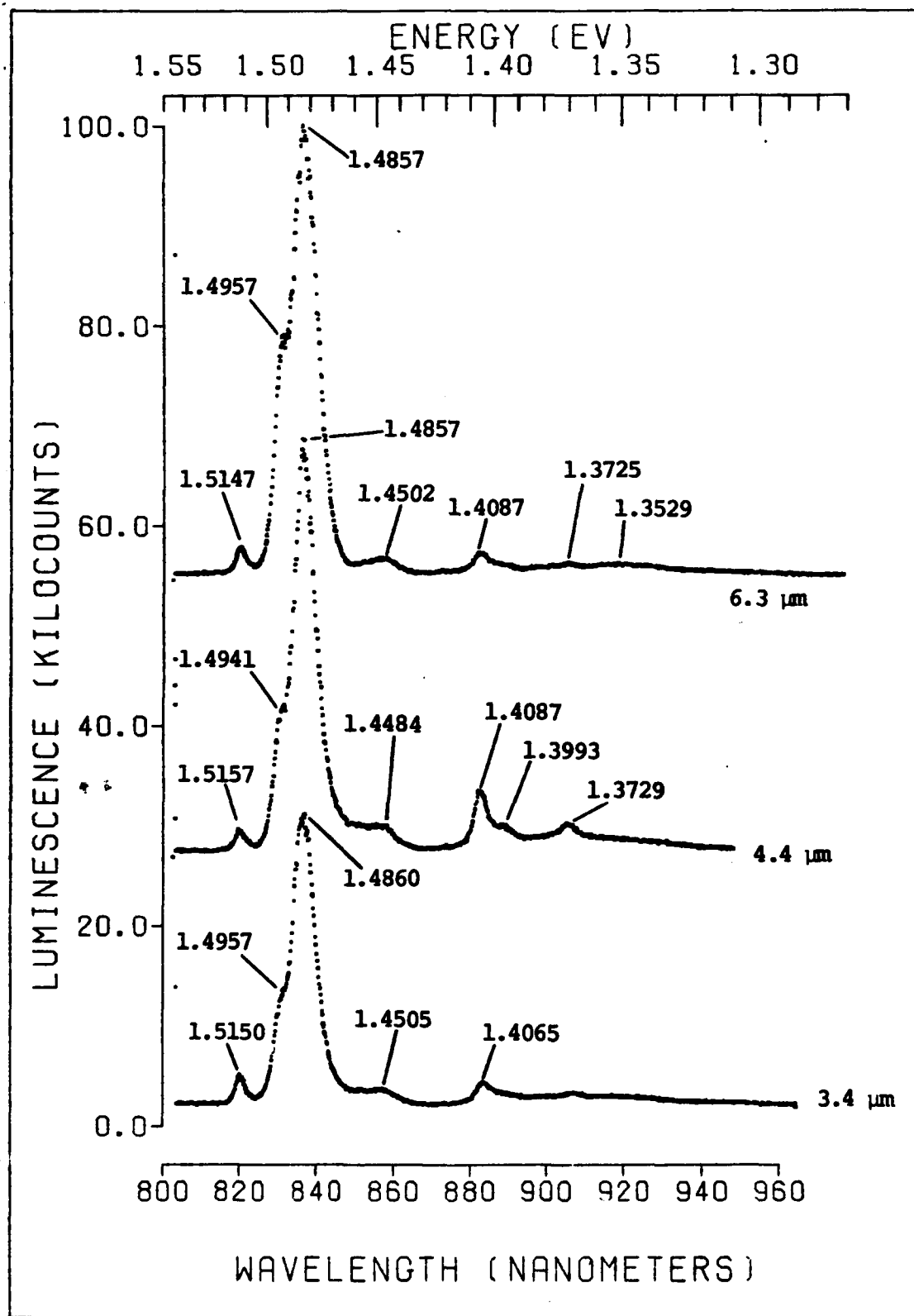
Figure 16. Expanded View of Figure 15

53

Figure 17. Depth Resolved Photoluminescence
of Sample Annealed at 950° C

55

the silicon acceptor peak reappears as the main peak at 1.4854 eV. The Zn_{Ga} peak (1.4876 eV) now appears as a shoulder on the high energy side of the main peak. The C_{As} peak (1.4946 eV) also appears as a shoulder on the high energy side of the main peak. The phonon replica of the Si_{As} peak is located at 1.4567 eV and the amplitude of the $V_{As}-Si_{As}$ peak (1.4071 eV) has been reduced by one-half. The Cu_{Ga} peak (1.3537 eV) and its LO phonon replica (1.3198 eV) are clearly visible. Figures 17 and 18 show the depth resolved photoluminescence spectra for the sample annealed at 950° C.

As mentioned previously, the sample annealed at 950° C displayed an unknown peak at 1.4827 eV. The position of this peak remains consistent until an etch depth of 3.4 μm. At this etch depth, the unknown peak is replaced by the Si_{As} peak (1.4860 eV). The C_{As} peak appears at 1.4957 eV. A phonon replica appears at 1.4505 eV. Due to its peculiar shape, this phonon replica may be a combination of phonon replicas of the C_{As} and Si_{As} peaks. At an etch depth of 4.4 μm, it appears that the Si_{As} peak (1.4857 eV) continues as the dominant peak. The C_{As} peak (1.4941 eV) appears as a shoulder on the high energy side of the main peak. A phonon replica appears at 1.4484 eV which, again, could be made up of phonon replicas due to the C_{As} and Si_{As} peaks. It is not known as to why the $V_{As}-Si_{As}$ peak (1.4087 eV) increases in amplitude at this etch depth. The As vacancy
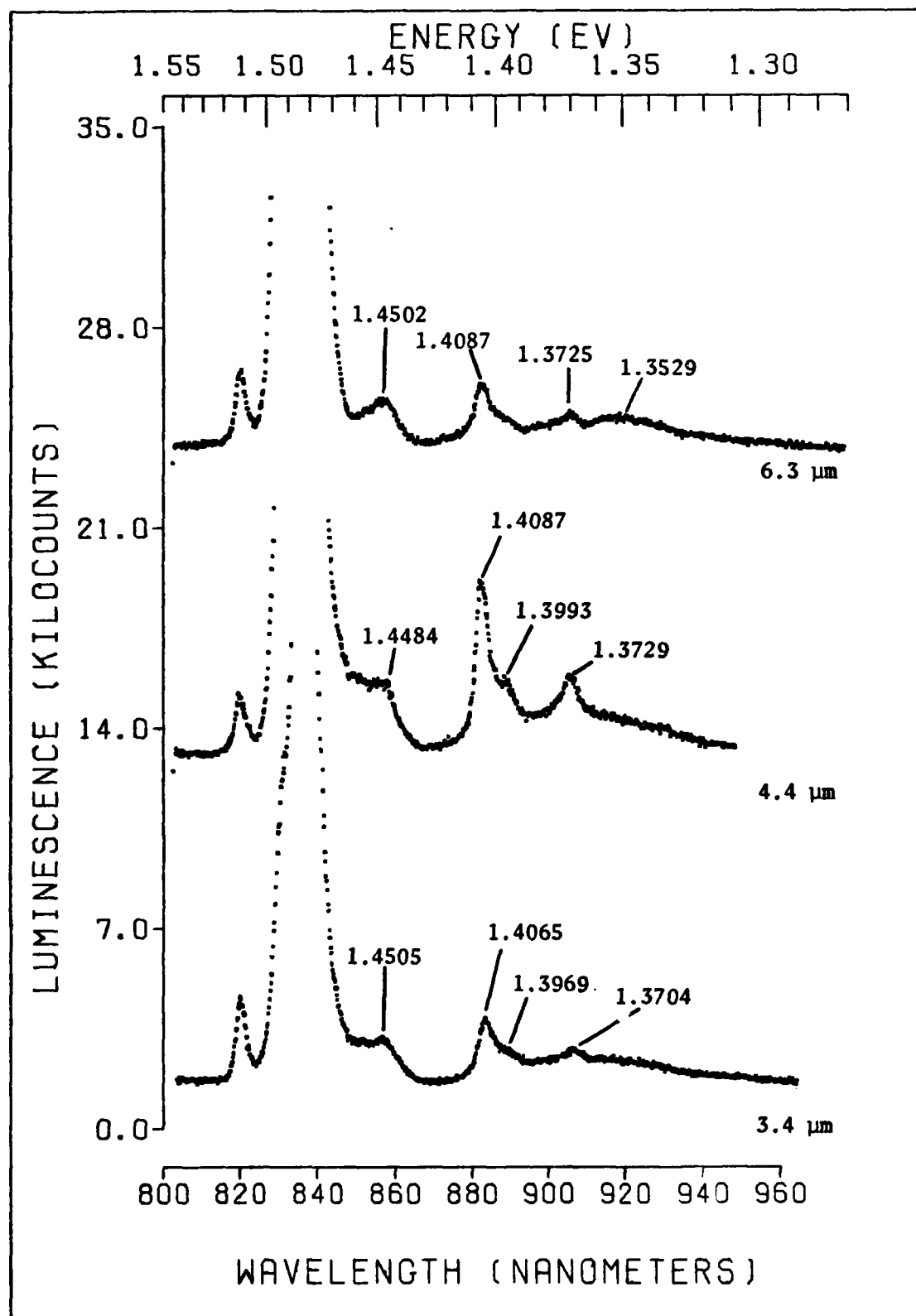
54

Figure 18. Expanded View of Figure 17

phonon replicas appear at 1.3993 eV and 1.3729 eV. The rest of the phonon replicas cannot be resolved. When the sample is etched 6.3 μm, it still appears that the main peak is due to Si_{As}. The carbon acceptor is located at 1.4957 eV, whereas the phonon replica of the Si_{As} peak is located at 1.4502 eV. The amplitude of the As vacancy peak (1.4087 eV) has decreased and its associated phonon replicas have disappeared. In their place, the Cu_{Ga} peak (1.3529 eV) has started to emerge.

Analysis of Results

The electrical profile measurements give a good indication as to the extent of the thermally converted layer. From the continued decrease in resistivity, Table 4 shows that the degree of thermal conversion increases from 850° C to 950° C. Therefore, it follows that the depth of the converted layer should also increase between 850° C and 950° C. This is evident from Tables 5 and 6, where the converted layer is largest for the sample annealed at 950° C. However, it is not evident from the photoluminescence spectra as to the nature of the thermal conversion mechanism. Instead, it is evident from the spectra that the samples have undergone some sort of change due to the heat treatments, but the relationship between these changes and thermal conversion is not clear. The changes that occur as a result of annealing will be discussed in the following paragraphs.

57

The unannealed samples clearly show a dominant Si acceptor peak and a carbon acceptor peak. Upon annealing, the Si_{As} peak is present only as a shoulder and the Zn_{Ga} peak becomes the dominant peak. The zinc acceptor peak continues to remain as the dominant peak until the 900° C anneal temperature is reached. At this temperature, the Si_{As} peak reappears as the dominant peak and the Zn_{Ga} peak is present only as a shoulder. At the 950° C anneal temperature, an unknown peak appears as the dominant peak. The energy of this peak is 1.4827 eV and does not correlate with any known impurity acceptor transitions. Furthermore, it should be noted that the luminescence of this peak is very strong. Other changes that occur in the photoluminescence spectra are the appearance of the Cu_{Ga} peak at 650° C, 700° C and 750° C and the growth of the V_{As}-Si_{As} peak at 850° C, 900° C, and 950° C. At these high anneal temperatures, the Cu_{Ga} peak either disappears or is lost under the As vacancy peaks.

From the depth resolved photoluminescence spectra of the sample annealed at 850° C, it can be seen that the Zn_{Ga} peak continues to remain as the dominant peak up to an etch depth of 3.9 μm. It is not known whether the Si_{As} peak reappears at a further etch depth.

For the sample annealed at 900° C, the Si_{As} peak continues to remain as the dominant peak up to an etch depth of 1.5 μm. At this point, the dominant peak switches from

58

Si_{As} to Zn_{Ga} and remains that way up to 7.5 μm into the material. At this point, the Si_{As} peak again becomes dominant. It is speculated that the inhomogeneous distribution of zinc and silicon impurities may cause the Si_{As} and Zn_{Ga} peaks to alternate in this manner. For the sample annealed at 950° C, the unknown peak (1.4827 eV) extends deep into the material. The Si_{As} peak returns as the dominant peak at an etch depth of 4.4 μm and continues as the dominant peak.

From the photoluminescence spectra, it can be seen that As vacancy generation increases as the anneal temperature increases from 850° C to 950° C. From the depth resolved photoluminescence, it is also evident that vacancy generation extends deep into the material. As these vacancies are etched away, the Cu_{Ga} peak is shown to reappear.

V. Conclusions and Recommendations

Conclusions

The purpose of this study was to characterize the mechanism causing n-type thermal conversion in chromium doped SI GaAs. From Van der Pauw Hall measurements, it was determined that n-type conversion occurred in samples annealed at 850° C, 900° C and 950° C. It was also determined that thermal conversion was more apt to occur at 900° C and 950° C rather than at 850° C. Electrical profile measurements showed that the converted layer is deeper for the sample annealed at 950° C than for the sample annealed at 900° C.

From the photoluminescence spectra of the samples, three predominant acceptor impurities can be singled out: zinc, carbon and silicon. The carbon and silicon acceptor peaks are present in the unannealed samples. At anneal temperatures below 850° C, the zinc acceptor becomes the predominant peak. At the 900° C anneal temperature, the silicon acceptor peak becomes the predominant peak. The depth resolved photoluminescence spectra at this anneal temperature show that the zinc and silicon peaks alternate as main peaks. This could be caused by an inhomogeneous distribution of zinc and silicon impurities. At the 950° C anneal temperature, an unknown peak appears as the dominant peak. The energy of this peak does not correlate with

established energies for conduction band-to-acceptor impurity transitions. This peak disappears after 3.4 μm of the material is removed. At that point, the silicon acceptor peak reappears as the predominant peak. It is not known whether the unknown peak has any bearing on the thermal conversion problem.

In conclusion, the mechanism for n-type thermal conversion could not be determined since no correlation existed between the electrical measurements and the photoluminescence spectra. It may well be that many of the impurities that contributed to thermal conversion were electrically active, but optically inactive.

Recommendations

The following recommendations are rendered concerning use of the system and for future studies in the area of n-type thermal conversion.

(1) The output beam of the laser should be beam expanded so that near uniform illumination of the sample is achieved. Beam expansion in this thesis was not possible due to low laser output power caused by a deteriorating laser tube.

(2) Spark source mass spectroscopy measurements, in conjunction with resistivity and photoluminescence measurements, may be helpful in correlating the surface layer with the impurity responsible for thermal conversion.

Bibliography

1. Air Force Avionics Laboratory. Characterization of III-V Semiconductors. Technical Report, TR-81-1036, April 1981.

2. Hallais, J., et al. "Properties and Thermal Conversion of Semi-Insulating GaAs," Institute of Physics Conference, 33b: 226-227 (April 1977).

3. Ohno, Hideo, et al. "Thermal Conversion Mechanism in Semi-Insulating GaAs," Journal of Applied Physics, 50(12): 8226-8228 (December 1979).

4. Pomrenke, Gernot S. "Photoluminescence of Undoped Semi-Insulating and Mg Implanted Indium Phosphide." MS Thesis. Wright-Patterson AFB, Ohio: School of Engineering, Air Force Institute of Technology, December 1979.

5. Edmond, J.T. "Heat Treatment of Gallium Arsenide," Journal of Applied Physics, 31(8): 1428-1430 (August 1960).

6. Wysocki, J.J. "Thermal Conversion in n-type GaAs," Journal of Applied Physics, 31(9): 1686-1687 (September 1960).

7. Lum, W.Y. and H.H. Wieder. "Thermal Degradation of Homoepitaxial GaAs Interface," Applied Physics Letters, 30(1): 1-3 (January 1977).

8. Lum, W.Y. and H.H. Wieder. "Thermally Converted Surface Layers in Semi-Insulating GaAs," Applied Physics Letters, 31(3): 213-216 (August 1977).

9. Zucca, R. "Effects of Heat Treatment on Semi-Insulating GaAs," Institute of Physics Conference, 33b: 228-235 (April 1977).

10. Koschel, W.H., et al. "Photoluminescence Studies of Surface Degradation on Semi-Insulating GaAs Substrates During the LPE Growth Cycle," Institute Physics Conference, 33a: 98-104 (1977).

11. Kasahara, J., et al. "Suppression of Thermal Conversion in Cr Doped Semi-Insulating GaAs," Journal of Applied Physics, 50(12): 8229-8231 (December 1979).

62

12. Klein, P.B., et al. "Thermal Conversion of GaAs," Journal of Applied Physics, 51(9): 4861-4868 (September 1980).

13. Anderson, John M. "Photoluminescence Study of Thermal Conversion in GaAs." MS Thesis. Wright-Patterson AFB, Ohio: School of Engineering, Air Force Institute of Technology, December 1981.

14. McKelvey, John P. Solid State and Semiconductor Physics. New York: Harper and Row, 1966.

15. Key, Manuel V. "Photoluminescence Study of Ion Implantation Damage in Gallium Arsenide." MS Thesis. Wright-Patterson AFB, Ohio: School of Engineering, Air Force Institute of Technology, December 1981.

16. Pankove, Jacque I. Optical Processes in Semi-Conductors. Englewood Cliffs NJ: Prentice-Hall, Inc., 1971.

17. Gorelenok, A.T., et al. "Temperature Dependence of the Impurity Photoluminescence of Cr-doped GaAs," Soviet Physics - Semiconductors, 5(1): 95-99 (July 1971).

18. Cronin, G.R. and R.W. Haisty. "The Preparation of SI GaAs by Cr Doping," Journal of the Electro-chemical Society, 874-877 (July 1964).

19. Williams, E.W., et al. "Photoluminescence II: Gallium Arsenide," Semiconductors and Semimetals, Volume 8, edited by R.K. Willardson and Albert C. Beer. New York: Academic Press, 1972.

20. Gershenzon, M. "Radiative Recombination in IV-V Compounds," Semiconductors and Semimetals, Volume 2, edited by R.K. Willardson and Albert C. Beer. New York: Academic Press, 1972.

21. Bogardus, E.H. and H.B. Bebb. "Bound-Exciton, Free to Bound, Band-Acceptor, Donor-Acceptor and Auger Recombination in GaAs," Physical Review, 176: 993-1002 (December 1968).

22. Pankove, J.I. "Electroluminescence," Topics in Applied Physics, Volume 17, New York: Springer-Verlag, 1977.

23. Pomrenke, Gernot S. "A Study of the 0.1 eV Conversion Acceptor in GaAs." Unpublished Paper. Air Force Avionics Laboratory: Wright-Patterson AFB, OH, undated.

24. Ashen, D.J., et al. "The Incorporation and Charac-
    terization of Acceptors in Epitaxial GaAs," Journal
    of Physical Chemical Solids, 36: 1041-1053 (February
    1975).

25. Hwang, C.J. "Photoluminescence Study of Thermal
    Conversion in GaAs Grown from Silica Boats," Journal
    of Applied Physics, 39(12): 5347-5356 (November 1968).

APPENDIX A

Element	Parts Per Million Atomic (ppma)
Be	< 0.01
B	< 0.01
C	≤ 0.1
O	< 0.02
Mg	< 0.03
Al	< 0.03
Si	0.1
S	< 0.03
Cr	0.3
Mn	0.03
Fe	0.3
Co	< 0.01
Ni	≤ 0.03
Cu	< 0.02
Zn	< 0.02
Ge	< 0.2
Se	< 0.2
Ag	< 0.02
Cd	< 0.04
Sn	< 0.03
Te	< 0.03
Au	< 0.01
Hg	< 0.03
Ti	0.1

TABLE A-1

Spark Source Mass Spectroscopy

for Sample E647-B-18

Vita

John A. Guillen was born on 17 January 1956 in
Elizabeth, New Jersey, the son of Joseph and Nieves Guillen.
He attended Irvington High School in Irvington, New Jersey.
Upon graduation in 1974, he entered the New Jersey Insti-
tute of Technology, formerly known as Newark College of
Engineering. He received his Bachelor of Science degree
in Electrical Engineering in 1978, along with a commission
in the United States Air Force. He was ordered to active
duty in August 1978 and was assigned to Rome Air Develop-
ment Center, Griffiss AFB, New York. In June 1981, he
was assigned to the School of Engineering, Air Force
Institute of Technology, Wright-Patterson Air Force Base,
Ohio.

Permanent Address:

Irvington, New Jersey

END

FILMED

3-83

DTIC